

2018

Development of a Silicon Diode Detector for Skin Dosimetry in Radiotherapy

Nikolina Vicoroski
University of Wollongong

Follow this and additional works at: <https://ro.uow.edu.au/theses1>

University of Wollongong

Copyright Warning

You may print or download ONE copy of this document for the purpose of your own research or study. The University does not authorise you to copy, communicate or otherwise make available electronically to any other person any copyright material contained on this site.

You are reminded of the following: This work is copyright. Apart from any use permitted under the Copyright Act 1968, no part of this work may be reproduced by any process, nor may any other exclusive right be exercised, without the permission of the author. Copyright owners are entitled to take legal action against persons who infringe their copyright. A reproduction of material that is protected by copyright may be a copyright infringement. A court may impose penalties and award damages in relation to offences and infringements relating to copyright material.

Higher penalties may apply, and higher damages may be awarded, for offences and infringements involving the conversion of material into digital or electronic form.

Unless otherwise indicated, the views expressed in this thesis are those of the author and do not necessarily represent the views of the University of Wollongong.

Recommended Citation

Vicoroski, Nikolina, Development of a Silicon Diode Detector for Skin Dosimetry in Radiotherapy, Master of Philosophy (Medical Radiation Physics) thesis, School of Physics, University of Wollongong, 2018.
<https://ro.uow.edu.au/theses1/223>

Research Online is the open access institutional repository for the University of Wollongong. For further information contact the UOW Library: research-pubs@uow.edu.au



Development of a Silicon Diode Detector for Skin Dosimetry in Radiotherapy

Nikolina Vicoroski

Supervisor:
Dr Marco Petasecca

This thesis is presented as part of the requirements for the conferral of the degree:

Master of Philosophy (Medical Radiation Physics)

The University of Wollongong
School of Physics

January 19, 2018

Declaration

I, Nikolina Vicoroski, declare that this thesis submitted in partial fulfilment of the requirements for the conferral of the degree Master of Philosophy (Medical Radiation Physics), from the University of Wollongong, is wholly my own work unless otherwise referenced or acknowledged. This document has not been submitted for qualifications at any other academic institution.

Nikolina Vicoroski

January 19, 2018

Abstract

The aim of in-vivo skin dosimetry is to measure the absorbed dose to the skin during radiotherapy, when treatment planning calculations cannot be relied on. It is of particularly importance in hypo-fractionated stereotactic modalities, where excessive dose can lead to severe skin toxicity. Currently commercial diodes for such applications are not available for medical physicists. In this study, we investigate a new detector for skin dosimetry based on a silicon epitaxial diode, referred to as the skin diode.

The skin diode is manufactured on a thin epitaxial layer and packaged using the “drop in” technology. It was characterised in terms of percentage depth dose, dose linearity and dose rate dependence and benchmarked against the Attix ionisation chamber. The response of the skin diode in the build-up region of the percentage depth dose (PDD) curve of a 6 MV clinical photon beam was investigated. Geant4 radiation transport simulations were used to model the PDD in order to estimate the water equivalent measurement depth (WED) of the skin diode. Measured output factors using the skin diode were compared with the MOSkin detector and EBT3 film at 10 cm depth at isocentre and at surface of a water equivalent phantom. The intrinsic angular response of the skin diode was also quantified in charge particle equilibrium conditions (CPE) and at the surface of a solid water phantom. Finally, the radiation hardness of the skin diode up to an accumulated dose of 80 kGy using photons from a Co-60 gamma source was evaluated.

The PDD curve measured with the skin diode was within 0.5% agreement of the Geant4 simulated curve. When placed at the phantom surface, the WED of the skin diode was estimated to be 0.075 ± 0.005 mm from Geant4 simulations and was confirmed using the response of a corrected Attix ionisation chamber placed at surface and having a water equivalent depth of 0.075 mm, with agreement to within 0.3%.

The output factor measurements at 10 cm depth were within 2% of those measured with film and the MOSkin detector down to a field size of $2 \times 2\text{cm}^2$. The dose response for all detector samples was linear with $R^2=1$ and with a repeatability within 0.2%. The skin diode intrinsic angular response showed a maximum deviation of 8% at 90 degrees and from 0 to 60 degree is less than 5%. The radiation sensitivity reduced by 25% after an accumulated dose of 20 kGy but after was found to stabilise. At 60 kGy total accumulated dose the response was within 2% of that measured at 20 kGy total accumulated dose.

This work characterises an innovative detector for in-vivo and real-time skin dose measurements that is based on an epitaxial silicon diode combined with the CMRP “drop in” packaging technology. The skin diode proved to have a water equivalent depth of measurement of $0.075 \pm 0.005\text{mm}$ and the ability to measure doses accurately relative to reference detectors.

Acknowledgments

I would firstly like to thank my principal supervisor Dr. Marco Petasecca for all his time and effort he has put towards this project. His dedication and commitment have been invaluable and greatly appreciate. I would also like to thank my co-supervisor Prof. Anatoly Rosenfeld for his support throughout this project.

I would like to show my appreciation to Dr Justin Davies for his support with irradiating the detectors at the GATRI facility (ANSTO) and A/Prof Martin Carolan and Dr Bradley Oborn for their supervision at the Wollongong Illawarra Cancer Care Centre while irradiating the silicon diode detectors. I would also like to thank FBK Trento for providing the n-type silicon epitaxial diodes for testing throughout the project.

I would like to extend my gratitude towards the following individuals who without their support and assistance this project would not have been possible:

- Anthony Espinoza
- Mitchell Duncan
- Prof. Peter Metcalfe
- A/Prof. Michael Lerch
- Vladimir Perevertaylo
- David Menichelli
- Peter Ihnat
- James Vohradsky
- Najdo Panovski

Finally a special thanks to my family, friends and especially my mum for supporting and encouraging me throughout my studies, your support was invaluable and I could not have done this without you.

Contents

Abstract	iii
List of Figures	viii
1 Introduction	1
2 Literature Review	4
2.1 Dosimetry	4
2.1.1 Dosimetric Quantities	4
2.1.2 Skin Dosimetry	7
2.1.3 In-Vivo Dosimetry	7
2.2 Detectors used in Dosimetry	8
2.2.1 TLD Devices	8
2.2.2 Ionisation Chambers	10
2.2.3 Radiosensitive Film	12
2.2.4 MOSFET	13
2.2.5 Diodes	15
2.3 Radiation Therapy	17
2.3.1 Introduction	17
2.3.2 Radiotherapy	18
2.3.3 High Energy Photons	19
2.3.4 Single Beam Linac	21
3 The Silicon Diode Detector and Readout Systems	24
3.1 Silicon Diode Detectors	25
3.1.1 Epi-5B	26
3.1.2 Epi-1C	27
3.2 Detector Packaging	28
3.3 Data Acquisition System	29
3.4 Irradiation by megavoltage medical linear accelerator	30
3.5 Attix Ionisation Chamber	32

4	Method	34
4.1	Radiation Hardness	34
4.2	Dose Linearity	36
4.3	Dose Per Pulse Dependence	36
4.4	Percentage Depth Dose	37
4.5	Output Factor and surface field size dependence	38
4.6	Angular dependence	39
5	Results and Discussion	41
5.1	Radiation Hardness	41
5.2	Dose Linearity	42
5.3	Dose per pulse dependence	43
5.4	Percentage Depth Dose	45
5.5	Output Factor and surface field size dependence	49
5.6	Angular dependence	52
6	Conclusion and Future Work	55
	Bibliography	57

List of Figures

2.1	Schematic representation of the different doses involved in in-vivo dosimetry for a single beam.[25]	20
3.1	Simplified top view diagram (not on scale) of the skin diode Epi-5B topology.	26
3.2	Simplified cross section view diagram (not on scale) of the skin diode Epi-5B topology.	26
3.3	Simplified top view diagram (not on scale) of the skin diode Epi-1C topology.	27
3.4	Simplified cross section view diagram (not on scale) of the skin diode Epi-1C topology.	27
3.5	Simplified schematic of the kapton pigtail cross section accommodating the skin diode die using the “drop-in” packaging technology.	29
3.6	Simplified block representation of experimental setup.	30
5.1	Response variation of the skin diode (Epi-5B) as a function of accumulated dose from a Co-60 gamma source.	42
5.2	Dose linearity response for the Epi-5B (squared symbol) and Epi-1C (dotted symbol) epitaxial silicon diodes.	43
5.3	Dose per pulse (DPP) response of the skin diode Epi-5B estimated at D_{max} (1.5cm) in solid water with a 6MV photon beam of 10×10 cm ² field size varying SSD from 100cm to 250cm.	44
5.4	Percentage Depth Dose measured by the skin diode in comparison to the Attix ionisation chamber with no build up cap and no correction factors applied.	46
5.5	Comparison of the same data set measured with Attix and Epi-5B with the simulations performed by the means of Geant4 in water and represented in logarithmic scale of the depth in water.	46
5.6	PDD measured by Epi-1C in comparison to Attix IC in a solid water phantom Epi-1C is “face up”.	48

5.7	PDD measured by Epi-1C in comparison to Attix IC in a solid water phantom Epi-5B is “face-down”	49
5.8	Output factor measured by MOSkin, EBT3 film and skin diode Epi-5B at 10cm depth in Virtual Water phantom.	51
5.9	Field size dependence of the skin diode placed at surface of the phantom in comparison with Attix with different build up thickness. . . .	51
5.10	Normalised intrinsic angular response of the skin diode placed in centre of a cylindrical PMMA phantom of radius of 15cm as a function of the angle. Center of the phantom is placed in isocentre. Normal incident angle is 0 degree.	53
5.11	Comparison of the normalized surface dose angular dependence measured by the skin diode , EBT3 film and Attix chamber at surface of a Virtual Water phantom for a 6MV photon beam.	54

Chapter 1

Introduction

In vivo dosimetry is the most direct method for monitoring the dose delivered to the patient receiving radiation therapy. Quality assurance of radiotherapy treatments involves several techniques and diversified approaches to verify that the dose delivered by the machine is accurate in intensity and position; in vivo dosimetry checks the dose delivered to the patient rather than the individual components prior to treatment.

Monitoring of the skin dose helps to prevent that an excessive dose is delivered to healthy tissues such as the skin. 20% of women undergoing 3D conformal radiotherapy for breast cancer treatments develop acute skin toxicity which dramatically affects the quality of life of the patient. [1]-[2] So ideally a dosimeter should be positioned at the point of interest inside a patients body or alternative on the surface. ICRP defines skin dose as the dose absorbed and measured at the water equivalent depth (WED) of 0.07mm [3] which makes estimation of skin dose challenging.

An ideal skin dosimeter should have extremely thin sensitive volume covered with tissue equivalent build-up providing a WED of 0.07 mm for skin dosimetry or even less if surface dose measurement is required.

Although the reference instrument for surface dosimetry at the air-to-water interface is the parallel plate extrapolation ion chamber, it is not used routinely for skin dosimetry. [4] The Attix ionisation chamber (IC) instead is often used for accurate surface dosimetry and correction factors used to correct the response to the skin WED. [5] Cylindrical IC are normally unsuitable for this application because of their large diameter, thick entrance window and large beam perturbation. Unguarded parallel plate ICs show an overresponse at very shallow depths due to the lateral secondary electrons scattering into the sensitive volume. [6]

For this reason, only large diameter ring-guarded ICs such as the Attix ionising chamber (Model 449 CNMC Co. Nashville, TN USA) are commonly considered as the reference instrument for interface dose measurement. Although very accurate for in-phantom measurements, the Attix IC can be used for skin dosimetry in a phantom only; they are limited to measure large field size beams of $5 \times 5\text{cm}^2$ and above [7] and they have been never manufactured in array for skin 2D dose mapping.

Radiochromic films have an excellent spatial resolution, tissue equivalency and can provide 2D dosimetric information. However, as radiochromic film is a passive detector, it does not allow for real-time measurements. Its response may also be affected by a WED of measurements much larger than 0.07mm [8], improper handling and scanner performance. [9]

Thermal Luminescence dosimeters (TLDs) have been used clinically for skin dose measurements in their carbon-loaded version. They are small in size and tissue equivalent however they require a long series of pre- and post-irradiation processes and a refined calibration procedure to be readout accurately. They are labour intensive and not real-time dosimeters, rendering them impractical for use in real-time in-vivo skin dosimetry. [10][11]

Zhuang and Olch showed that a nano-dot Optically Stimulated Luminescence Dosimeter can be adopted as skin dosimeter with stabilisation delay of less than 10minutes after irradiation. However it has an effective WED of 0.8mm which is larger than WED of 0.07mm accepted for skin dosimetry. [12]

Semiconductor detectors such as MOSFETs are able to achieve excellent spatial resolution because of their high sensitivity and small sensitive volumes. The MOSkin, based on the MOSFET technology and recently introduced by CMRP, are also able to produce real time readout and provide a reproducible water equivalent depth of dose measurement of 0.07 mm. [13] MOSkin has demonstrated good agreement with the Attix IC for surface dose measurements and angular dependence in MV and kVp photon beams. [14] However, due to their limited linear dynamic range (up to 50Gy) they are not practical to use in a 2D array.

Silicon diode detectors could represent a good candidate to develop a new technology to measure in real-time in vivo skin dose. The technology development of silicon diodes makes them the standard reference dosimeter for a variety of application in radiotherapy from quality assurance of stereotactic modalities to in-vivo dosimetry due to their small size allowing for high spatial resolution and high sensitivity. [15][16] However, current designs of silicon diodes die and packaging, which provides electronic equilibrium conditions for MV field of interest, do not make them suitable for direct skin dosimetry on medical linacs.

The purpose of this thesis is to perform a full characterisation of a silicon epitaxial diode detector for surface dosimetry in a phantom. The experimentation involved includes: (i) detector calibration, linearity and reproducibility; (ii) percentage depth dose; (iii) field size dependence; (iv) angular dependence, (v) dose per pulse dependence and (vi) radiation hardness. In order to provide consistency and reliability the results were compared with Monte Carlo simulations, ionisation chambers and film.

Research Outcome of the thesis:

Publication: N. Vicoroski(1), A. Espinoza(1), M. Duncan(1), B. Oborn(2), M. Carolan(1,2), P. Metcalfe(1,4), M.L.F. Lerch(1,4), D. Menichelli(3), V.L. Perevertaylo(5), A.B. Rosenfeld(1,4), M. Petasecca(1,4),*

- (1) Centre for Medical Radiation Physics, University of Wollongong, Wollongong, Australia
- (2) Illawarra Cancer Care Centre, Wollongong Hospital, Wollongong, Australia
- (3) IBA Dosimetry GmbH, Schwarzenbruck, Germany
- (4) Illawarra Health and Medical Research Institute IHMRI, Wollongong, Australia
- (5) SPA BIT, Kiev, Ukraine

“Development of a Silicon Diode Detector for Skin Dosimetry in Radiotherapy”
Medical Physics (accepted for publication 15/06/2017).

Chapter 2

Literature Review

2.1 Dosimetry

Radiation dosimeter is a device that measures absorbed dose resulting from interactions of ionising radiation with matter. It is the determination of radiologically relevant quantities such as exposure, KERMA, fluence, dose equivalent, energy imparted and so on. A dosimeter along with its reader is referred to as a dosimetry system. The use of modern radiotherapy techniques such as EBRT (External Beam Radiation Therapy) requires a new generation of radiation dosimeters that can be used for in vivo skin dosimetric purposes and are able to provide real-time dosimetric information whilst being small in size and volume.[17][18]

2.1.1 Dosimetric Quantities

Absorbed dose is a non-stochastic quantity that applies to both indirectly and directly ionising radiations. In the case of indirectly ionising radiations, the energy is imparted to matter in a two-step process. The first step results in kerma, a mechanism by which indirectly ionising radiation transfers energy as kinetic energy to secondary charged particles. The second step results in absorbed dose where the charges particles will transfer some of their kinetic energy to the medium and thus lose some of their energy in the form of radiative losses through Bremsstrahlung. Absorbed dose is related to the stochastic quantity energy imparted, which can be defined as the mean energy (ϵ) imparted by ionising radiation to matter of mass (m) in a finite volume (V) by:

$$D = \frac{d\epsilon}{dm} \tag{2.1}$$

The energy imparted (ϵ) is the sum of all the energy entering the volume of interest minus all the energy leaving the volume, taking into account any mass energy conversion within the volume. $d\epsilon$ is the energy imparted on an infinitesimal volume dV , with dm being a mass in dv . Pair production decreases the energy by 1.022MeV, while electron-positron annihilation increases the energy by the same amount. Absorbed dose has units of Gray (Gy), where 1Gy is the absorption of 1J/kg (Joule/kilogram) of matter.[19]

The International Commission on Radiological Protection (ICRP) defines equivalent dose as a “limiting quantity” in which exposure limits are specified to ensure that “the occurrence of stochastic health effects is kept below unacceptable levels and that tissue reactions are avoided”. [20] It is a measure of the radiation dose to tissue where an attempt has been made to allow for the different relative biological effects of different types of ionising radiation which is shown in table 2.1.[21]

Radiation Type	Radiation weighting factor, w_R
Photons	1
Electrons and muons	1
Protons and charged pions	2
Alpha particles, fission fragments, heavy ions	20
Neutrons	Continuous function of neutron energy

Table 2.1: Recommended radiation weighting factors.

It is impractical to measure equivalent dose, thus calculated values may be used to compare the equivalent dose with observed health effects. The equivalent dose is calculated as a sum taken over all types of radiation doses. The absorbed dose deposited in the body tissue or organ, T , is multiplied by the radiation weighting factor, w_R , which is dependent on the type and energy of the radiation, R . This then takes into account the contributions of the varying biological effect of different radiation types. This is shown in the equation:[20]

$$H_T = \sum_R w_R D_{(T,R)} \quad (2.2)$$

Where:

H_T is the equivalent dose absorbed by tissue, T .

$D_{T,R}$ is the absorbed dose in tissue, T , by radiation type, R .

w_R is the radiation weighting factor defined by regulation.

Since w_R is dimensionless, the unit for the equivalent dose is the same as for absorbed dose, J/kg however with a special name of Sieverts, Sv.[20]

Effective dose can be defined by ICRP as the sum of the equivalent doses in the principal tissues and organs in the body, each weighted by a tissue weighting factor, w_T . This weighting factor takes account of the probability of fatal cancer, the probability of non-fatal cancer, weighted for severity, and the average length of life lost due to an induced cancer [22].

ICRP emphasises that the effective dose provides a measure of radiation detriment for protection purposes only. It does not provide an individual-specific dose and should not be used for epidemiological evaluations [20].

The recommended tissue weighting factors are defined in table 2.2.

Tissue	Tissue weighting factor w_T	Sum of w_T values
Bone-marrow (red), colon, lung, stomach, breast, remainder tissues*	0.12	0.72
Gonads	0.08	0.08
Bladder, oesophagus, liver, thyroid	0.04	0.16
Bone surface, brain, salivary glands, skin	0.01	0.04
Total:		1.00

Table 2.2: Recommended tissue weighting factors [20].

*Remainder tissues: Adrenals, extrathoracic (ET) region, gall bladder, heart, kidneys, lymphatic nodes, muscle, oral mucosa, pancreas, prostate (male), small intestines, spleen, thymus, uterus/cervix (female).

Effective dose can be calculated through the sum of the equivalent doses in all specified tissues and organs of the body which can be shown through the equations below:

$$E = \sum_T W_T \sum_R W_R D_{T,R} \quad (2.3)$$

$$E = \sum_T W_T H_T \quad (2.4)$$

Where:

H_T or $W_R D_{T,R}$ is the equivalent dose in a tissue or organ, T.

W_T is the tissue weighting factor.

Effective dose and absorbed dose have the same units J/kg which is given the name Sieverts, Sv.[20]

2.1.2 Skin Dosimetry

The skin is the largest organ in the body and is very sensitive to radiation. The most sensitive part of the skin is the epidermis and the basal layer of the epidermis which is located at 0.07mm below the skin surface. According to ICRP publication 59 [3] this is considered to comprise the most radiosensitive epithelial cells. It is essential that potential early and late effects of the radiotherapy treatment are assessed accurately to limit exposure to normal tissue from unnecessary irradiation. Therefore an ideal in vivo dosimeter should possess the following characteristics:[13]

- (i) tissue equivalent;
- (ii) being re-usable;
- (iii) small in physical size and has a small sensitive volume;
- (iv) features (eg temperature, energy) which are consistent and characterisable;
- (v) does not perturb the radiation field;
- (vi) non-hazardous to humans;
- (vii) deliver accurate and reliable dose results at the required depth and
- (viii) able to provide real-time dosimetric information.

2.1.3 In-Vivo Dosimetry

In radiotherapy in-vivo dosimetry is the measurement of the radiation dose that is received by the patient during treatment. In-vivo dosimetry in external beam radiotherapy, is performed on the surface of the patients body to measure entrance dose and skin dose. It is the most direct method for monitoring the dose delivered to the patient and is a useful tool for quality assurance. It is able to detect major errors associated with dosimetric errors such as human error in data generations and data transfer and also equipment malfunctioning, assess clinically relevant differences between planned and delivered dose, record dose received by individual patients, and fulfil legal requirements. A well-developed in-vivo dosimetry plan will provide precautions without significantly extending treatment delivery time.[10][23]

In-vivo dosimetry can also be used to monitor irradiation for special techniques such as total body irradiation or total skin electron irradiation. Recommendations regarding radiation dose delivery are provided by the International Commission of Radiation Units and Measurements (ICRU) stating that the radiation dose to be delivered should be within 5% of the prescribed dose. It is thus recommended that

the total error in dose delivered at the end of the planning and treatment “chain” should be less than 5%.[24]

In-vivo dosimeters can be divided into two categories: real-time detectors and passive detectors. These two types of dosimeters require a calibration that is generally obtained by comparing their response against a calibrated ionisation chamber (IC) in a known radiation field. Most of these detectors have a response that is energy and/or dose rate dependent and consequently require adjustments of the response to account for changes in the actual radiation conditions compared to the calibration situation. Correction factors should be taken into account due to these dependencies: changes in field size, source-detector distance, temperature, pressure and orientation, and including the presence of a build-up cap. More so the presence of a build-up cap is important for detectors that are used for entrance or exit IVD (in vivo dosimetry). Special attention should be paid to the selection of appropriate build-up cap material and thickness for entrance dose measurements during EBRT as the dose beneath the dosimeter may be significantly attenuated by the dosimeter build-up material. For that reason entrance dose measurements are often limited to a few fractions. Furthermore when moving away from the reference conditions the material and thickness of the build-up cap has an effect on the magnitude of correction factors.[10]

2.2 Detectors used in Dosimetry

2.2.1 TLD Devices

Thermoluminescence is a thermally activated phosphorescence. It is widely known for the number of different ionising radiation induced by a thermally activated phenomena. [19] Thermoluminescence dosimetry is based on imperfect crystals being able to absorb and store the energy of ionising radiation, which upon heating is re-emitted in the form of electromagnetic radiation, mainly in the visible wavelength spectrum. The light is emitted then detected by a photomultiplier and correlated to the absorbed dose received by the TL material.[25]

The energy states in the crystal are represented with energy increasing upwards along the ordinate. Free electrons and holes are produced under the irradiation effect and both of them are free to travel through the solid in the conduction band for a short period of time. They may be ultimately trapped at defects, or fall back into the valence band and recombine either radiatively (fluorescence) or non-radiatively with holes, or be captured at luminescent centres with the emission of

light. The states just below the conduction band are the electron traps, and the states just above the valence band are hole traps. The trapping levels are empty before irradiation. The electrons may stay in the traps for prolonged periods, which confer to the thermoluminescent method, the advantage of storage of information. The information can then be collected by heating the crystal to a temperature depending on its nature.

During irradiation the secondary charged particles lift electrons into the conduction band either from the valence band, which leaves a free hole in the valence band, or from an empty hole trap, which fills the hole trap. The system may approach thermal equilibrium through several means:

- (i) free charge carriers recombine with the recombination energy converted into heat;
- (ii) a free charge carrier recombines with a charge carrier of opposite sign trapped at a luminescence centre, the recombination energy being emitted as optical fluorescence;
- (iii) the free charge carrier becomes trapped at a storage trap, and this event is then responsible for phosphorescence or the thermoluminescence and OSL processes.[25]

For in-vivo measurements TL detectors have the advantage of being highly sensitive under a small volume and do not have to be connected to an electrometer with a cable. Their major disadvantage is the time required for readout which can be considerably decreased by a good choice of equipment and a good methodology.[25]

TLD has become popular due to ease of use on the patient and the small physical size of the dosimeter. They are particularly useful for measuring point doses, given their small size and that information is stored permanently. However for surface dose measurements with TLDs the thickness of the cover layer won't allow one to obtain the dose at a depth of 0.07mm, which is a potential disadvantage given the importance of depth for a skin dose measurement. To combat this, a method of extrapolation can be employed. By simultaneously using several thicknesses of TLD the data collected from each can be drawn on to extrapolate the dose to the required depth. Another technique for measuring skin dose is by using carbon loaded ("black") TLDs. The advantage of the black TLDs is the carbon absorbs all light emitted within the TLD, except at the shallow surface layer. This can be adjusted to suit the required depth of 0.07mm, thus facilitating the measurement of surface doses.[25]

The disadvantage of using TLDs is they require advance notice for sample preparation; frequent calibration is necessary, and TLDs are somewhat sensitive to environmental conditions. TLDs also do not allow immediate readout, and they require a lengthy annealing procedure. This makes their use time consuming during radiotherapy. Further, the reproducibility of TLD measurements is relatively poor, which requires several TLDs being irradiated and averaged, thus increasing the resources required. [26]

2.2.2 Ionisation Chambers

Ionisation chambers are widely used in radiotherapy and in diagnostic radiology for the determination of radiation dose. They have gained popularity due to their small variation in response to energy, dose, dose rate and reproducibility[27] making them the benchmark for calibration and comparison of other dosimeter detectors. More so the size of some ionisation chambers makes them undesirable for measuring small or narrow fields as the lack of lateral electronic equilibrium and the volume of the chamber perturb the field of interest. [27] Thus making them undesirable as an in-vivo dosimeter as they will show inaccurate results. Ionisation chambers require a power supply which can be in excess of 200V for the ionised charge collection and patient safety restricts them to use of phantoms only. [27]

Ionisation chambers come in various shapes and sizes depending on the specific requirements; some include cylindrical (thimble type, eg Farmer type), parallel-plate (e.g. Attix), and extrapolation chambers. The general characteristics for the various ionisation chambers are a gas filled cavity that is surrounded by a conductive outer wall which has two collecting electrodes: the anode and the cathode where the anode is positively charged with respect to the cathode. The presence of radiation will cause the charged particles to traverse the gas inside the ionisation chamber creating ion pairs. The voltage potential applied across the chamber will cause the electron of each ion pair to move to the anode while the positively charged gas atom or molecule will move to the cathode thus creating an electronic pulse. These individual pulses are too small to be detected and thus multiple radiation interactions are easily detectable. An insulating layer is present in between the wall and the collecting electrodes to reduce any current leakage when the polarised voltage is applied. The accumulated charge is proportional to the energy of the incident particles. [19][28]

Cylindrical ionisation chambers are used for point-dose measurements in megavoltage photon radiation therapy due to their excellent stability, linear response to absorbed dose, small directional dependence, beam-quality response independence, and traceability to a primary calibration standard. The cylindrical ionisation chambers minimise the sensitivity response variation as a function of beam entry angle when the beam central axis is perpendicular to the chamber axis of symmetry.[29]

A parallel plate ionisation chamber is recommended for electron beam dosimetry for energies below 10MeV. It is also used for surface dose and depth dose measurements in the build-up region of photon beams however at the expense of directional dependence in the case of full charged particle equilibrium. [19] The Attix parallel-plate ionisation chamber is flat and very thin at 4.8mg/cm^2 (25microns), with only 2mm separation between the plates. [30] The advantage that the Attix parallel-plate ionisation chamber has over other chambers is the large guard ring that reduces over-response due to low energy electrons to less than 1%. [31][32]

Extrapolation chambers are parallel-plate chambers with a variable volume and are used for surface dose measurements in orthovoltage and megavoltage x-ray beams and in the dosimetry of beta rays and low energy x-rays. They can also be used in absolute radiation dosimetry when it is directly embedded into a tissue equivalent phantom. Cavity perturbation for electrons can be eliminated by making measurements as a function of the cavity thickness and extrapolating to zero thickness. The perturbation can be estimated by through using parallel-plate chambers of finite thickness. [19]

To determine whether an ionisation chamber is functioning adequately, it should be able to demonstrate a stable response over time where it can be compared against a local secondary standard ionisation chamber for quality assurance purposes.[29]

Throughout the experiment, the Attix parallel-plate ionisation chamber was used as the benchmark standard for comparing different dosimeters.

2.2.3 Radiosensitive Film

Film is capable of revealing a 2D dose map with good spatial resolution while ionisation chambers only display a point dose. Therefore, film is useful in radiation dosimetry to observe dose distribution for treatment or for quality assurance testing of the dose uniformity provided by the linear accelerator. There are two commercially available options for 2D film dosimetry, which are radiographic and radiochromic film.

Radiographic film serves as a radiation detector and a relative dosimeter that is used for diagnostic radiology, radiotherapy and radiation protection. It provides excellent 2D spatial resolution and in a single exposure provides information about the spatial distribution of the radiation in the area of interest or the attenuation of radiation by intervening object. [19]

Radiographic film is coated with silver bromide (AgBr) uniformly on one or both sides of the base. When x-rays, gamma rays or light strike the grains of sensitive AgBr, the Br⁻ ions are liberated and captured by the Ag⁺ ions creating a visual change in the film where the interaction took place. The degree of colour change of the film is proportional to the amount of ionising radiation interacting with the film at specific locations. Through this visualisation the cross sectional profile of the beam that is being used can be seen. Radiographic film encounters some disadvantages in that it does not allow for any real time dose measurements, the useful dose range is limited, film batches can vary in sensitivity due to production processes and the energy dependence is pronounced for lower energy photons up to 14-20 times more than compared to high energy photons. [29]. Even though there are some present weaknesses with radiographic film it does present a convenient option for two-dimensional dosimetry with its high spatial resolution and inexpensive compared to radiochromic film. [28]

Radiochromic film is used in radiotherapy dosimetry, with the most common being GafChromic film, which is colourless with a nearly tissue equivalent composition of 9% hydrogen, 60.6% carbon, 11.2% nitrogen and 19.2% oxygen that develops into a blue colour upon exposure to radiation. [19] The film becomes polymerised as it absorbs the light, displaying a blue effect on the film which is then detectable by a densitometer. The effective depth of measurement for GafChromic film was determined to be 0.153mm[33] which is larger than the required depth of 0.07mm for skin dosimetry radiotherapy. However with appropriate correction, which is dependent on field size, skin dosimetry of 0.07mm can be achieved.[33] It has a high resolution and can be used in high dose gradient regions for dosimetry. In addition radiochromic film has a few advantages over radiographic film in the ease of

usage through the elimination of the need for darkroom facilities, film cassettes or film processing as they are self-developing, dose rate independence, better energy characteristics (except for low energy x-rays of 25kV or less), and insensitivity to ambient conditions. [19].

2.2.4 MOSFET

A metal-oxide semiconductor field effect transistor (MOSFET) dosimeter is similar to diodes in that they belong to the same category of semiconductor detectors and are built on a silicon substrate. It can be used for in-vivo dosimetry as it has a water equivalent depth (WED) similar to that of the sensitive layer of the skin at 0.07mm. MOSFETs consist of three electrical terminals: a source, drain and gate. The source and drain are made from highly doped silicon n or p-type which depends on the material of the substrate, if the source and drain are p-type silicon then the substrate will be n-type silicon and thus called a p-channel MOSFET and vice versa for n-channel MOSFET. [34] The gate, which is the third terminal, is on top of an insulating silicon dioxide layer and underneath that layer is the silicon substrate.[25]

Where a MOSFET dosimeter is used, the threshold voltage (V_{TH}), which is a sufficiently negative voltage is applied at the gate, can be determined when the bias voltage is applied between the source and drain terminals in order to allow a predetermined current, I_{ds} , to flow. During irradiation of the MOSFET the gate is kept at a positive bias which results in a charge separation effect in which the electrons will tend towards the gate and the holes tend towards the Si-SiO₂ interface. Due to the electrons being considerably faster, they will escape the gate contact while the majority of the holes will remain at the Si-SiO₂ interface and thus captured in traps to produce a positive thin charge layer.[35][36][37]

Through this exposure to ionising radiation the holes, in relation to the electron-hole pairs, are permanently trapped which will cause an alteration to the threshold voltage. The threshold voltage should be recorded before and after irradiation in order to demonstrate a voltage shift.

When a higher bias is applied during irradiation it will result in a larger proportion of charges being collected, thus increasing the sensitivity of the device. The sensitivity of the device is independent of the temperature during irradiation. As the bias/sensitivity is increased the total dose that is able to be recorded before the device is saturated and no longer useful is reduced. Hence when the MOSFET becomes saturated through over exposure of ionising radiation it will no longer produce

accurate and reliable results thus resulting in a limited lifespan. [19][25]

The advantages of the MOSFETs are:[25]

- Relatively immediate response.
- No need for cables to connect the detectors on the patient to an electrometer; however the gate must then be pre-biased before the irradiation.
- Small size (of the order of 1mm^3).
- Good reproducibility: 2-3%.
- Non-destructive readout: possibility of study of dose accumulation over the different treatment session, however with a fading correction.
- Response independent of dose-rate.
- Negligible angular dependence ($\pm 2\%$ for 360 degrees).

The disadvantages of the MOSFETs are:[25]

- Response dependent on temperature except for dual base dosimeters; their principle consists of associating 2 detectors with a different grid voltage and of displaying the difference in their signals in order to produce temperature compensated dosimeters.
- Response decrease as a function of accumulated dose, resulting in a limited lifetime of the detector (of the order of 10^2 Gy in the usual conditions).
- Response dependent on energy: as for diodes, the basic material of a MOSFET is silicon so that a similar energy dependence is observed.
- Slight loss of charge after irradiation: readings to be taken always at the same time delay after termination of the irradiation.

A MOSFET-based dosimeter which was designed and prototyped by the Centre for Medical Radiation Physics (CMRP) at the University Of Wollongong (UOW) is known as the MOSkin detector. This detector is very similar to that of the usual MOSFET detectors in that it is able to measure skin dose at 0.07mm, provides real-time response, and built-in temperature compensation, which makes it suitable for in-vivo skin dosimetry measurement. The design and packaging of the MOSkin address issues within the traditional MOSFET dosimeters and improve the quality and efficiency for clinical in-vivo skin dosimetry radiotherapy.

2.2.5 Diodes

The operation of semiconductor diode dosimeters detectors are comparable to ionisation chambers however they are generally used without an external bias voltage and are more sensitive for the same detection volume.[25]

Diodes that are used for in-vivo radiotherapy dosimetry are typically silicon detectors and provide an advantage of immediate signal availability. [25] These diodes are produced by taking n-type or p-type silicon and counter-doping the surface to produce the opposite type material. The density of silicon and the low average energy required to form a carrier pair in silicon results in a radiation current density which is about 18,000 times that of air. This allows a small volume (approx. 10^{-2} - 10^{-1} mm³) of the silicon diode to produce an easily measured current, [16] as a result diodes have a high sensitivity. Due to silicon having a considerably high atomic number of 14, the diode detectors will lead to a greater sensitivity to low-energy photons, as the photoelectric effect cross-section is approximately proportional to Z^5 . Therefore diode detectors should be used for small-field dose distribution measurements where there are relatively few low-energy photons.[28]

The low-energy sensitivity of the diode can be reduced through introducing a low-energy filter or shield within the construction of the diode; such a setup is referred to as an “energy-compensated” diode detector. The key structure of the silicon diodes is the p-n junction. The n-type silicon diode detectors are doped with impurities of a pentavalent element such as phosphorous which are called “donor” elements. Each of these donor elements contribute a free electron to the silicon thus the majority carriers are the electrons and the minority carriers are the holes in an n-type silicon diode detector. The p-type silicon diode detectors are doped with impurities of a trivalent element such as boron which are called “acceptor” elements. Each of these acceptor elements accept an electron that results in a mobile hole in the silicon which is equivalent to a positively charged carrier. The majority carriers are the holes and the minority carriers are the electrons in a p-type silicon diode detector. Therefore p-type silicon diodes are formed by the donor impurities being doped into a p-type substrate and the n-type silicon diodes are doped with acceptor impurities in the n-type substrate. This creates a direct contact between the p- and n-side of the diode. The majority carriers from each side will diffuse to the opposite side such that electrons on the n-side will diffuse to the p-side leaving behind positively charged donor ions, while the holes on the p-side will diffuse to the n-side leaving negatively charged acceptor ions behind.[16] Through the transition between both regions of p-type and n-type material a charge-free “depletion layer” is formed in which an electrostatic potential difference is created which is about

0.7V for a silicon diode. Hence as a result an electric field, E , is created over the depletion layer and the diode will operate in an “unbiased” or “short-circuit” mode as no external bias is applied to the diode to reduce leakage current [25]

As the diode becomes irradiated “electron-hole” pairs are created in the depletion layer. Additionally, due to the high doping levels at the n-side of a p-type diode, an abundant of crystal imperfections or “recombination centres” are present at that side, which leads to a high probability of recombination for the holes. As a result only the minority charge carriers, which are electrons in this case, will contribute to the ionisation signal. Due to this process the charge equilibrium between n- and p-sides of the diode are disrupted by the radiation.

The signal generated by the diode detectors originates mostly from secondary electrons, which are produced by the incoming radiation beam outside the detectors active volume where different materials create different quantities of secondary electrons. Silicon diodes that are commercially available are found to have a large change in sensitivity with the angle of incidence of radiation typically up to $\pm 25\%$, which is undesirable for dosimetry applications as it limits accuracy.

This creates a larger problem if the measured surface has an irregular shape, which will cause the front of the diode to be oblique to the incident direction of radiation. This will prohibit the use of this type of diode in any type of arc therapy. In addition, a similar problem occurs if there is significant scattered dose from adjacent surfaces. [15][38]

In-vivo dosimetry diodes are provided with build-up encapsulation that must be appropriately chosen depending on the type and quality of a specific clinical beam. The build-up cap used should guarantee that the detector is measuring under electron equilibrium conditions. Insufficient build-up requires the application of large correction factors that can influence the accuracy of in-vivo dose measurements. [23] Silicon diodes offer many advantages for in-vivo dosimetry, such as real-time read-out, high sensitivity, simple instrumentation, reliability and robustness. However diode plus build-up cap response is subject to a number of influence factors that need to be corrected for, such as the dependence of the signal on the dose rate, the varying response with irradiation angle, and the energy dependence of the response. Even for small variations in the spectral composition of radiation beams the diode response may change, which is important for the measurement of entrance and exit dose. Diodes show also a variation in response with temperature, however some IVD diode systems provide for automatic patient temperature compensation. Another disadvantage might be the need to handle the cables connecting the diodes on the patient with the electrometer located outside the treatment room. However,

in newer systems this problem has been overcome with wireless technology. Diodes change their sensitivity after having accumulated sufficiently large doses and have to be recalibrated regularly through a period of clinical use. [10]

2.3 Radiation Therapy

2.3.1 Introduction

Radiation therapy has been long recognised as an effective method for treating cancer and depends on the accurate delivery of the absorbed dose in the patient. The goal of radiotherapy, regardless of the delivery method, is to destroy the cancerous DNA structures whilst minimising damage to normal healthy tissue, thus causing the cells to die or to reproduce slowly or to cause mutations so future generations fail to reproduce.[39]

IMRT is an advanced radiation delivery technique however is not the only one. Other systems that are currently used are Tomotherapy, VMAT (Volumetric Modulated Arc Therapy), Rapid Arc, Gamma Knife and CyberKnife which are able to deliver high dose/short fractionation course radiotherapy. All these systems have the potential of delivering high skin dose.

The radiation dose is a prescription of dose depending upon the location and type of cancerous tissue delivered to the patient in the specified target area. This prescription of dose must minimise exposure to surrounding normal structures to thus prevent any side effects.[39]

Radiation therapy utilises a range of beam spectra for treatment of specific tumours with different energies. It can be delivered externally through external beam radiation therapy machines or internally through placing a radioactive material inside the patient near the cancerous cells known as brachytherapy. External beam radiation therapy can be classified through use of the energy of the beam being utilised. Orthovoltage/superficial x-rays utilise the range of 30-500keV and are generally used for superficial, small tumours such as skin cancers as the lower photon energies increase the photoelectric cross section and the probability of the photoelectric effect interaction is greater, thus decreasing the penetrability of the beam. Alternatively megavoltage x-rays within the range of 4-18MeV can be used for tumours located deeper within the body at depths inaccessible for orthovoltage x-rays to reach. Hence through increasing the range of the x-ray energies it also increases the depth at which the maximum radiation dose is deposited. [28][40] A typical radiation oncology department will treat about 80% of its patients with various external

beam techniques and about 10-20% of its patients with brachytherapy.[19]

The basic principle of conformal radiotherapy is that tumour control can be improved by using special techniques that allow the delivery of a higher tumour dose while maintaining an acceptable level of normal tissue complications in comparison to standard dose delivery techniques. Intensity Modulated Radiation Therapy (IMRT) is a type of conformal radiotherapy whereby the radiation dose volume is conformed to the PTV while at the same time keeping the dose to specified organs at risk below their tolerance dose. The conformal radiotherapy chain is based on 3D target localisation, 3D treatment planning and 3D dose delivery techniques. Therefore this allows increased tumour control probability and decreased treatment morbidity (i.e. decreased normal tissue complication probability (NTCP)). Target localisation is achieved through anatomical and functional imaging such as CT, MRI, single photon emission computer tomography (SPECT), PET and ultrasounds. The treatment planning system for IMRT is achieved through inverse planning which uses intensity modulated beams to improve target dose homogeneity and spare organs at risk, compared with standard forward planning techniques which design uniform intensity beams shaped to the geometrical projection of the target. In forward planning based treatment planning system (TPS), the user establishes beam directions, size and weight and the software produces Dose Volume Histograms based on the beams arrangement. However in inverse planning bases TPS, the user sets dose-volume constraints and priorities and the software optimizes the beam ballistics that better meets these requirements. Dose can be delivery through intensity modulated non-coplanar beams produced with multileaf collimators (MLCs). [19] A MLC will adjust the size and shape of the radiation beam by adjusting the metal leaves, usually made from tungsten, to block out areas and filter others to vary the beam intensity and precisely distribute the radiation dosage.[19]

Although IMRT is a more precise delivery technique than other available techniques. Any kind of radiation therapy carries with it inherit risks due to the nature of the treatment. As such quality assurance (QA) and equipment verification systems are necessary in order to detect a malfunctioning medical accelerator or human error during the planning phase or patient treatment. [41] It ensures consistency of the medical prescription and safe fulfilment of that prescription, regarding the dose of the target volume, together with minimal dose to normal tissue, minimal exposure of personnel and adequate patient monitoring aimed at determining the end result of the treatment. [19]

2.3.2 Radiotherapy

External photon beam radiotherapy is usually carried out with more than one radiation beam in order to achieve a uniform dose distribution inside the target volume and an as low as possible a dose in healthy tissues surrounding the target. ICRU Report No.50 [42] recommends a target dose uniformity within +7% and -5% of the dose delivered to a well-defined prescription point within the target. Modern photon beam radiotherapy is carried out with a variety of beam energies and field sizes under one of two set-up conventions: a constant source to surface distance (SSD) for all beams, or an isocentric set-up with a constant source to axis distance (SAD). In an SSD set-up the distance from the source to the surface of the patient is kept constant for all beams, while for an SAD set-up the centre of the target volume is placed at the machine isocenter. Clinical photon beam energies range from superficial (30-80kVp), through orthovoltage (100-300kVp), to megavoltage energies (Co-60 - 25MV). Field sizes range from small circular fields used in radiosurgery, through standard rectangular and irregular fields, to very large fields used for total body irradiation (TBI). [19]

2.3.3 High Energy Photons

The characterisation of a dosimeter is performed when the condition of charged particle equilibrium (CPE) exists. Charged particle equilibrium (CPE) exists for the volume (V) if each charged particle of a given type and energy leaving the volume is replaced by an identical particle of the same energy entering the volume. [17] Evidently when radiation equilibrium exists so does CPE, and the existence of radiation equilibrium is a sufficient condition for CPE to exist. However for in-vivo skin dosimetry detectors, the dosimeter should be characterised on the surface of the patient instead of at the depth of maximum dose (d_{max}). The reason for such characterisation of a dosimeter is due to the dosimetric condition of skin surface and the build-up region being different to the dosimetric conditions at the depth of maximum dose. There is a notable steep dose gradient in the build-up region at the interface of two media (air and human tissue), which indicates that CPE does not exist.[13]

As a single photon beam propagates through air or a vacuum it is governed by the inverse square law, however as the photon beam transmits through a phantom or patient it is not only affected by the inverse square law, but also by attenuation and scattering of the photon beam. Thus a direct measurement of the dose distribution inside the patient is a complicated process and essentially impossible, yet for a

successful outcome of patient radiation treatment it is imperative that the dose distribution in the irradiated volume be known precisely and accurately. This can be achieved through the use of several functions that link the dose at any arbitrary point inside the patient to the known dose at the beam calibration (or reference) point in a phantom. A typical dose distribution on the central axis of a megavoltage photon beam striking a patient can be shown in Figure 2.1 with several points and regions identified. The beam enters the patient on the surface, where it delivers a certain surface dose, $D_{surface}$, defined at 0.05cm below the entrance surface. $D_{surface}$ increases rapidly until it reaches the entrance dose ($D_{entrance}$) that is defined as d_{max} . The target dose (D_{target}) is defined at the depth of dose specification which is equal to the mean of $D_{entrance}$ and D_{exit} . The dose then decreases almost exponentially until it reaches the exit dose (D_{exit}) which is a value defined as the patients exit point. The exit dose definition implies conditions of complete electron backscatter as the d_{max} is larger than the electron backscatter range (s), however smaller than the photon backscatter range (r).[19]

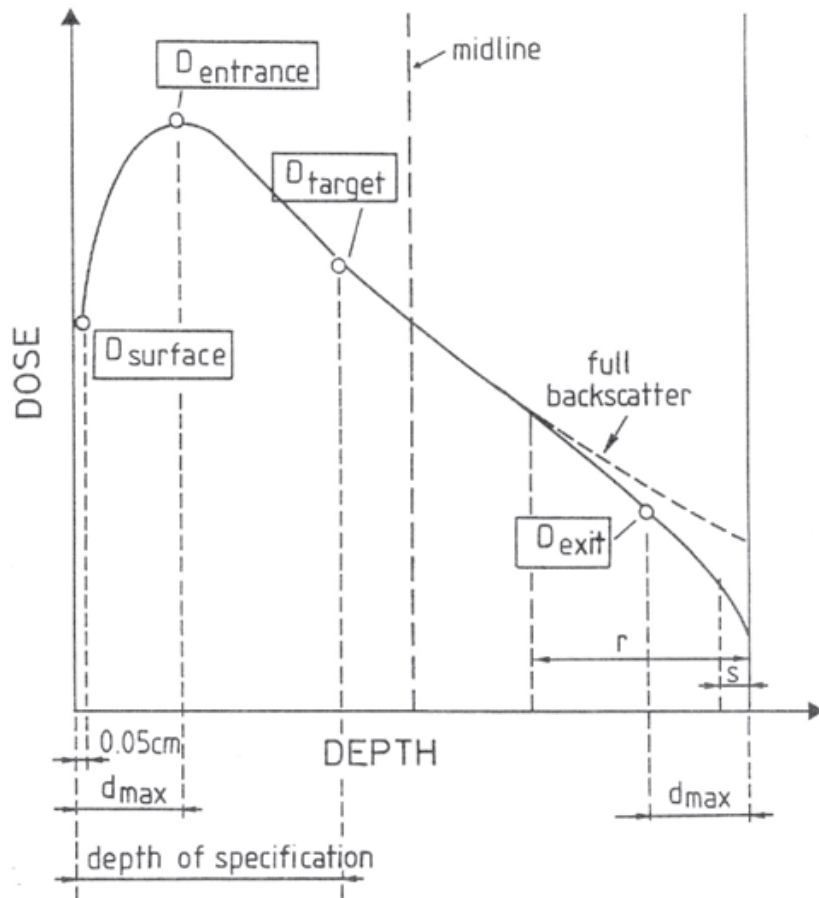


Figure 2.1: Schematic representation of the different doses involved in in-vivo dosimetry for a single beam.[25]

2.3.4 Single Beam Linac

Entrance Beam

The dose at which the entrance side of a medium is irradiated by a single photon beam will gradually increase from a low value at the surface up to a maximum value $D_{entrance}$ at a depth of d_{max} . This increase is dependent upon a number of values such as the energy, the opening of the collimator, the skin-to-source distance (SSD), the introduction of beam modifying devices and the distance separating them from the patient skin etc. The increase of a dose as a function of depth from surface to d_{max} is steepest just below the surface and it gets less pronounced at larger depths until it reaches d_{max} thereafter decreasing. Thus this relationship indicates that the measurement of $D_{entrance}$ should be conducted with enough material in front and around the detector placed at skin level in order to be reproducible.[25]

The detectors used for in-vivo dosimetry have a sensitive layer approximately 1mm thick or less which indicates that when they are used on the skin the detector will integrate the dose in a region of very steep dose gradient complicating the ratio between dose to the detector and $D_{entrance}$. However, when a bare detector is used it is subject to almost the full headscatter contaminating electron spectrum thus the number of electrons increase as a function of the collimator opening and decrease as a function of SSD. In order to limit the influence of headscatter electrons on $D_{entrance}$, build-up caps are introduced with dimensions relative to the dimensions necessary to ensure full build-up for the smallest collimator opening in the absence of any accessory. Despite this, an issue can arise with higher energies as the thickness of the build-up cap can be several centimeters of tissue-equivalent material thus compromising the patient comfort and leading to an underdosage of the treatment volume, combined with loss of skin sparing in large areas.

A way to reduce the build-up cap dimensions is to use a high density material and all precautions should be taken to avoid errors and uncertainties such as calibrating the detector with the build-up caps.

Incomplete build-up on an entrance detector might lead to certain correction factors which are only determined by the influence of the headscatter electron contamination and not at all by the intrinsic characteristics of the detector type involved. [25]

Exit Beam

The dose delivered to the patient at the beam exit point is referred to as the exit dose. At the exit side of the patient there is a build-down region related to lack of backscatter radiation from the air behind the patient. Thus producing a dose distribution curve that slightly decreases from the extrapolated dose distribution curve. This lack of backscatter concerns photons as well as secondary electrons. While the lack of electron backscatter causes a build-down of the dose only in the latter few millimetres in front of the exit surface of the patient (approximately from 1mm for Co-60 to 3mm for 20MV x-rays, Lambert et al 1983), the lack of photon backscatter influences a much deeper region and increases as a function of field size. This relatively small effect is attributed to the missing scatter contribution at the exit point from points beyond the exit dose.[25]

To derive the exit dose D_{exit} at d_{max} from the exit detector signal, it is necessary to cover the detector with enough material behind and around it in order to ensure complete electron backscatter (otherwise it would be too high a dose gradient, which would decrease the accuracy). The ratio between the dose to the detector and the exit dose has to be determined in a phantom in the same irradiation conditions as for the patient. Mostly the in-vivo measurement of the exit dose is performed concomitantly with that of the entrance dose. It is then important when positioning the exit detector to avoid the shadowing effect of the entrance detector. [19][25]

Surface Dose

The surface dose for megavoltage photon beams is generally much lower than the maximum dose which occurs at depth d_{max} , and depends on the beam energy and field size. The larger the photon beam energy, the lower the surface dose, which for a $10 \times 10 \text{ cm}^2$ field typically amounts to some 30% of the maximum dose for a cobalt beam, 15% for a 6MV x-ray beam and 10% for an 18MV x-ray beam. Thus the surface dose increases with field size for a given beam energy. To measure the dose to the skin which is defined at 0.05cm under the surface (ICRU, 1984) thin detectors must be used. When the detectors are thin, such as monocoated photographic emulsions, they should be covered with about 0.05cm of build-up material. However for thick detectors, such as TL chips or thin layer of TL powder wrapped in envelopes made of paper, they are to be placed on the skin without any build-up material. Also correction factors have to be applied to their response when their effective point of measurement is not at 0.05cm under their surface (Kron et al 1993). The surface dose is measured with thin window parallel- plate ionisation chambers for both polarities, with the average reading between the positive and negative polarities

taken as the surface dose value. The surface dose represents contributions to the dose from: [19][25]

- Photons scattered from the collimators, flattening filter and air;
- Photons backscattered from the patient;
- High energy electrons produced by photon interactions in air and any shielding structures in the vicinity of the patient.

Build-up region

The build-up region results from the relatively long range of energetic secondary charged particles (electrons and positrons) that are first released in the patient by photon interactions (photoelectric effect, Compton effect, pair production) and then impart their kinetic energy in the patient. The region immediately beneath the patients surface, is where the condition of CPE does not exist and the absorbed dose is much smaller than the collision kerma. However as the depth, z , increases, CPE is eventually reached at $z=z_{max}$ where z is approximately equal to the range of secondary charged particles and the dose becomes comparable with the collision kerma. Beyond z_{max} both the dose and collision kerma decrease due to the photon attenuation in the patient, resulting a transient rather than true CPE. [19]

The build-up of absorbed dose is responsible for the skin sparing effect in the case of high energy photon beams. However, in practice the surface dose is small and does not equal zero due to the electron contamination in the beam from the photon interactions in the media upstream from the phantom or due to charged particles generated in the accelerator head and beam modifying devices.[19]

Depth of Dose Maximum

The depth of dose maximum z_{max} beneath the patients surface depends on the beam energy and beam field size. The beam energy dependence is the main effect; the field size dependence is often ignored as it represents only a minor effect. Nominal values for z_{max} range from zero for superficial and orthovoltage x-ray beams, through 0.5cm for Co-60 beams, to 5cm for 25MV beams.[19]

For a given beam energy, the largest z_{max} occurs for fields of $5 \times 5\text{cm}^2$. For fields larger than $5 \times 5\text{cm}^2$, z_{max} decreases due to collimator scatter effects (cobalt units) and collimator and flattening filter scatter effects (for linacs). For fields smaller than $5 \times 5\text{cm}^2$, z_{max} decreases due to phantom scatter effects.[19]

Chapter 3

The Silicon Diode Detector and Readout Systems

Diodes are represented as a two-terminal device, in that two electrodes are required for a connection. [16] The two terminals of the diode can be connected to a coaxial cable in two different configurations that result in either a positive or negative signal from the diode detector. A negative diode detector is made by connecting the centre conductor of the cable to the cathode of the diode, while a positive diode detector connects the centre conductor to the anode of the diode. This choice does not affect the performance of the detector and is made by the manufacturer to match the input polarity requirement of the electrometer. [16] In the case of this experiment, the diodes are constructed to provide a positive signal.

The silicon material in the diode is commonly referred to as the “die”. The construction of the die, including size, the composition of the doping, the forming of the p-n junction by diffusion and any lattice defects, either initially present or caused by irradiation, determine some of the characteristics of the detector response to radiation. The use of silicon as a material to be used as a radiation detector for in vivo dosimetry provide some desirable characteristics. The features of silicon include a low ionisation energy (3.6eV/pair) [43] indicating that a decent signal can be obtained due to the sensitivity being high. There is a linear relationship between the charged particle energy crossing the diode and the electron/hole pairs produced along the track of the particle. Also, silicon has a long mean free path which allows for good charge collection efficiency as there is a higher probability of the carrier reaching the diode if created in the depletion region. [43]

As the diode becomes irradiated “electron-hole” pairs are created in the depletion layer and due to the high doping levels at the n-side of a p-type diode, an abundant amount of crystal imperfections or “recombination centres” are present at that side, which leads to a high probability of recombination for the holes.[25] As a result only the minority charge carriers, which are electrons in this case, will contribute to the ionisation signal and due to this process the charge equilibrium between n- and p-sides of the diode are disrupted by the radiation. Thus, when connecting both sides externally to each other, a current will be detected at radiation, which when the diode is in the unbiased mode, is proportional to the number of electron-hole pairs produced i.e. to the dose. [25]

The characterisation of dosimeters is normally performed where the charged particle equilibrium (CPE) condition exists. [16][44][45]

However, characterisation of a skin dosimeter should be performed at the surface and at very shallow depth in a build-up region where strong electronic disequilibrium and steep dose gradient exist. Such conditions are typical for in vivo skin dosimetry. [13]

3.1 Silicon Diode Detectors

The diodes that are used in this analysis are both silicon diode detectors of different structures and composition p-type and n-type from CMRP at UOW and Fondazione Bruno Kessler (FBK - Trento, Italy), respectively.

It is indicated that p-type diodes suffer less sensitivity loss as a function of accumulated dose than their n-type counterparts and are said to be less dose-rate dependent. [46] However n-type detectors are recently being modified to adapt the characteristics for in vivo measurements. Thus, it can be determined from the experiments, that are to follow, that the n-type silicon diode detector is an ideal in vivo dosimeter.

3.1.1 Epi-5B

Two epitaxial diodes were fabricated. The skin diode (named Epi-5B) was fabricated by Fondazione Bruno Kessler (FBK - Trento, Italy) on an n-type silicon $5\mu\text{m}$ thick epitaxial layer grown on a $0.001\Omega\text{-cm}$ n-type silicon substrate. The detector structure is represented in Figure 3.1 and is composed of boron implanted P+ sensitive area of $0.5 \times 0.5\text{mm}^2$, with a total size of the die of $0.75 \times 0.75\text{mm}^2$. The effects of the superficial leakage current are minimised by using a guard-ring surrounding the entire pixel sensitive area.

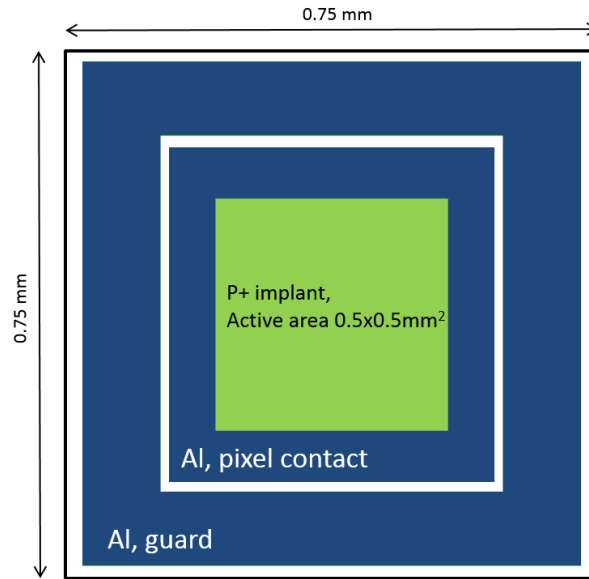


Figure 3.1: Simplified top view diagram (not on scale) of the skin diode Epi-5B topology.

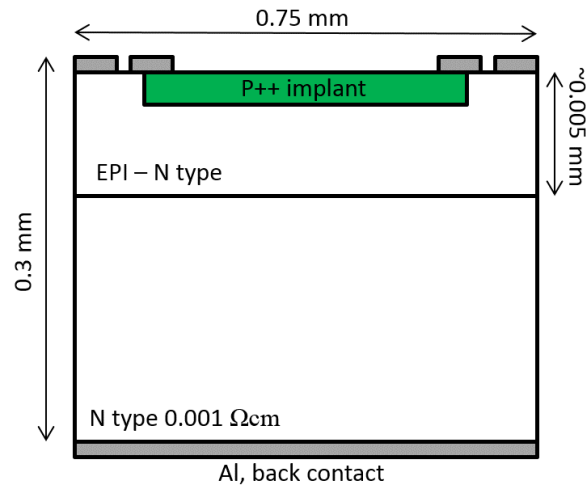


Figure 3.2: Simplified cross section view diagram (not on scale) of the skin diode Epi-5B topology.

3.1.2 Epi-1C

To estimate the effect of the thickness of the epitaxial layer (sensitive volume) on WED of dose measurement an epitaxial silicon diode was fabricated on a P-type silicon $50\mu\text{m}$ thick epitaxial layer is grown on a $0.001\Omega\text{-cm}$ P-type silicon substrate (named Epi-1C see Figure 3.3). The Epi-1C has N+ phosphorus implanted active area of $0.6 \times 0.6\text{mm}^2$ and overall die dimensions of $1.5 \times 1.5\text{mm}^2$. This diode has been adopted for the fabrication of the 11×11 2D diode array MagicPlate. [13]

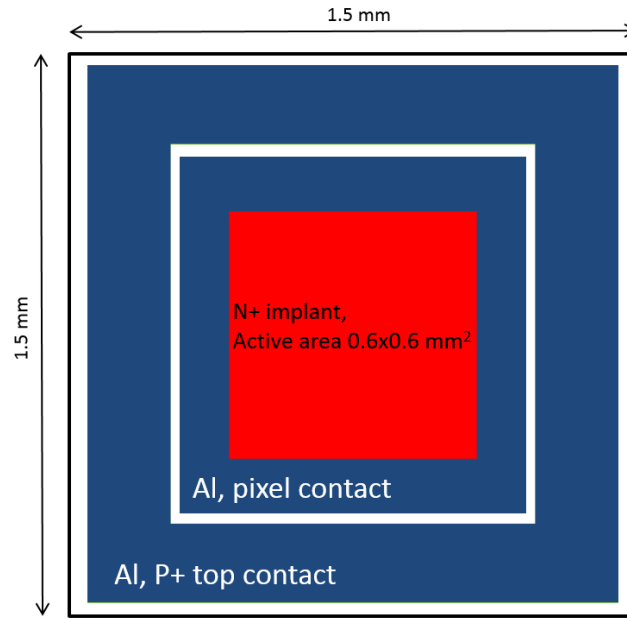


Figure 3.3: Simplified top view diagram (not on scale) of the skin diode Epi-1C topology.

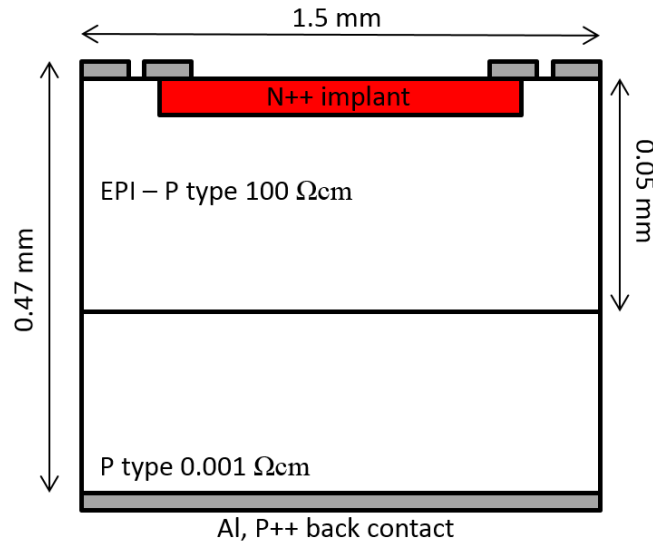


Figure 3.4: Simplified cross section view diagram (not on scale) of the skin diode Epi-1C topology.

Both these detectors were used for in vivo dosimetry experimentation and were covered with Kapton tape material for both protection and build-up. The build-up cap is used to guarantee that the detector is measuring under electron equilibrium conditions. If there is insufficient build-up, this can influence the accuracy of in vivo dose measurements, and large correction factors are to be implemented. [47]

More so both diodes had the presence of deep energy-level defects and trapped charged at the Si-SiO₂ interfaces, which also increases the leakage current. However, this effect is often mitigated by using the silicon detector in passive mode or unbiased.

3.2 Detector Packaging

Both epitaxial diodes have been embedded in Kapton pigtails with $0.6 \times 3\text{mm}^2$ cross section and 350mm length using CMRP proprietary “drop-in” packaging technology. “Drop-in” technology is a technique developed by the Centre for Medical Radiation Physics (CMRP), University of Wollongong to design a dosimetric tool to be used for Intensity Modulated Radiation Therapy (IMRT/VMAT) quality assurance.

This packaging technique is based on tab bonding of the silicon die underneath a stack of polyamide and aluminium layers as illustrated in Figure 3.5. Therefore, the build-up material thickness above the detector sensitive layer is reproducible and providing WED of approximately 0.07mm. [48] The “drop-in” technology is compatible with standard flexible printed circuit manufacturing technologies and avoids the use of high atomic number materials for packaging of semiconductor radiation detectors, minimising the perturbation of the beam. The Kapton pigtail outside of the diode is shielded by a thin aluminium foil and grounded to minimise radio-frequency interference. [49] Further details on the “drop-in” packaging technology can be found elsewhere.[14][38]

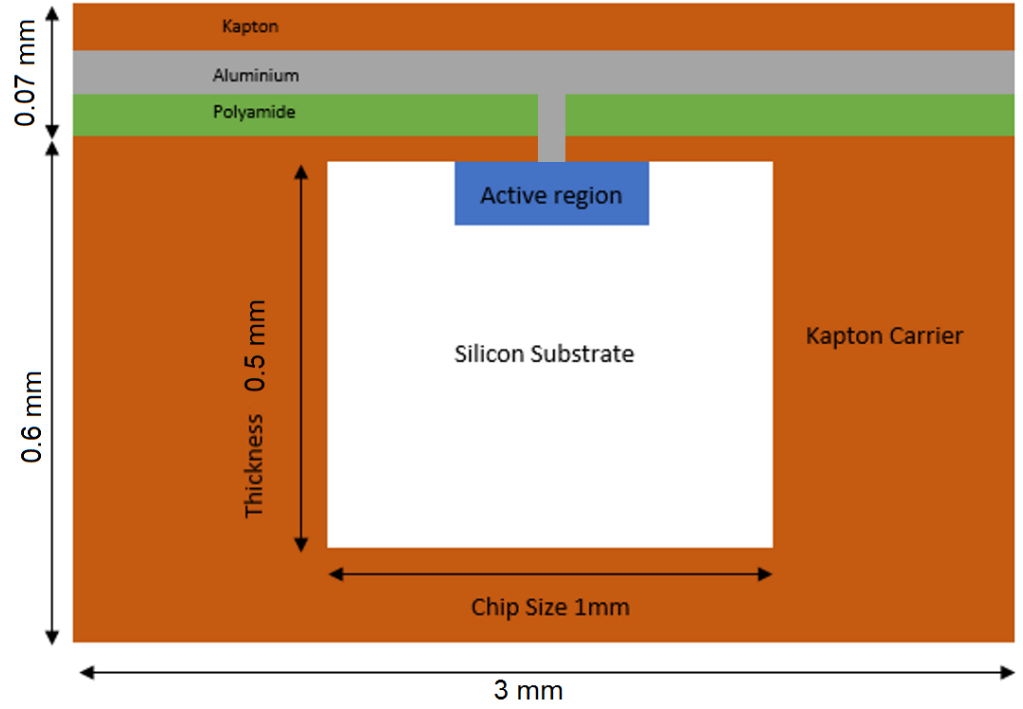


Figure 3.5: Simplified schematic of the kapton pigtail cross section accommodating the skin diode die using the “drop-in” packaging technology.

3.3 Data Acquisition System

The data acquisition system (DAS) used throughout the experiments enables the detector channels to be read in real-time and across a wide dynamic range with high linearity. It reads out the charge generated by the radiation beam into the sensitive volume of the diodes and is based on multichannel electrometer connected to a front-end which feeds the analogue to the digital data converters.

The extremely thin sensitive volume adopted for the skin diode Epi-5B requires the use of a high sensitivity electrometer. The multichannel electrometer used for this work is based on the AFE0064 which is a 64-channel analogue front end designed and commercialised by Texas Instruments [50] to readout flat panel amorphous silicon detectors. The AFE0064 is equipped with a double sampler for subtraction of the baseline, which is a feature that has been adopted in this work for accurate measurements of the charge collected in the volume of $1.25 \times 10^{-3} \text{ mm}^3$ of the epitaxial diode.

The AFE0064 presents also a major advantage to be able to sample the detector only when the beam is on, by the synchronisation of the detector sampling and the analogue to digital conversion with the LINAC synch signal. Through this modality it has a double advantage of minimising the effects of electronic noise and parasitic current, and managing the dead time by reading out the data while the beam is off.

It allows to read out integral charge on a 16-bit scale of 4.8pC, which corresponds to measured charge resolution of 7e-5pC. The electrometer is read out by a USB 2.0 interface managed by a graphical interface installed into a standard laptop. For further details on the electrometer architecture, please refer to [41].

Figure 3.6 displays a block diagram of the experimental setup depicting the communication between the computer and the detector being used.

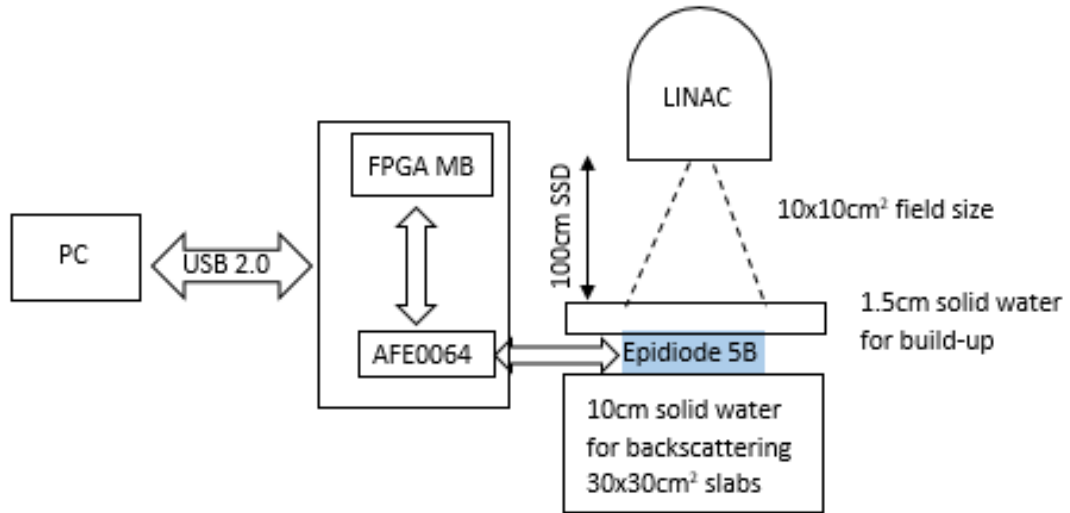


Figure 3.6: Simplified block representation of experimental setup.

3.4 Irradiation by megavoltage medical linear accelerator

The measurements conducted were performed using the Varian Clinac 21Xi machine at the Illawarra Cancer Care Centre of Wollongong Hospital (NSW, Australia) equipped with a multi-leaf collimator (MLC) Millennium-120 for 6MV photon beams with a flattening filter. The linear accelerator utilises electromagnetic fields to propel charged particles to high energies. At the treatment head, the charged particles are directed to a target consisting of a high Z number (such as tungsten), and the subsequent radiation is directed through a series of collimators to deliver a precise dose to the target volume. [51]

The Linac was used to conduct the following measurements:

- Linearity of the detector over varying dose;
- Percentage Depth Dose of the detector;
- Dose Per Pulse Dependence of the detector;
- Angular Dependence;
- Output factor;

An ideal in-vivo diode dosimeter would display the following characteristics:

- (i) Thin enough to determine dose delivered to shallow depths;
- (ii) Resistance to radiation damage;
- (iii) Reproducibility of WED (packaging);
- (vi) Wide dynamic range;
- (v) Linear dose response;
- (vi) Insensitive to dose rate variations;
- (vii) Energy and temperature independent;
- (viii) Able to provide real-time dosimetric information.

The epitaxial diode detectors were irradiated with a Co-60 source at the Australian Nuclear Science and Technology Organisation (ANSTO, Lucas Heights, NSW, Australia) to study the effects of radiation damage on charge collection efficiency. The effect of radiation damage on the degradation of radiation sensitivity of Epi-1C epitaxial diode is presented in [52]. Reference [52] demonstrates the improvement of the efficiency and long term stability of silicon dosimeters obtained by an n+ -p junction surrounded by a guard-ring structure implanted on an epitaxial p-type Si layer grown on a Czochralski substrate. The sensitivity of devices made up on 50 μ m thick epitaxial Si degrades by only 7% after an irradiation with 6MeV electrons up to 1.5kGy, and shows no significant further decay up to 10kGy. The passive epitaxial diode is usually less affected by accumulated dose due to the thin, sensitive volume.

To stabilise the skin diodes response, they were pre-irradiated with dose increments of 20kGy up to a total accumulated dose of 80kGy with response measured at each irradiation step. The radiation damage caused by continuous radiation is the same as pulsed radiation. The response of the skin diodes is measured under standard conditions by delivering 100MU on 6MV linear accelerator photon beam, field

size of $10 \times 10\text{cm}^2$, at depth 1.5cm in a solid water phantom at a source to surface distance (SSD) of 100cm. The error bars are calculated as one standard deviation over five repetitions of the same measurement.

3.5 Attix Ionisation Chamber

Ionisation chambers are considered the reference tool for calibration and comparison of other dosimeter detectors in radiotherapy. The reason behind their popularity is due to their small variation in response to energy, dose, dose rate and their high reproducibility. [27] However measuring small or narrow fields becomes a challenge when using ionisation chambers as the lack of lateral electronic equilibrium and the volume of the chamber perturbs the field.

Ionisation chambers have been extensively investigated over the years in particular by Das et al (2008) and the Institute of Physics and Engineering in Medicine about structure and function.

The ionisation chamber that is used in this work is the Attix ionisation chamber. The reason for using a parallel plate ionisation chamber over a cylindrical or Markus ionisation chamber is that the Attix ionisation chamber is flat and thin with dimensions of $4.8\text{mg}/\text{cm}^3$ and with the front electrode consisting of 0.025mm Kapton conductive film and coating, and 2mm separation between the electrode plates. [53][54] The Attix ionisation chamber provides a suitable geometry for surface dosimetry, although at the expense of directional dependence in the case of full charged particle equilibrium. The Attix ionisation chamber has a large guard-ring 13.5mm wide that reduces the over-response in the build-up region to less than 1%. [55]

The table 3.1 shows the differences between a Cylindrical, Parallel-Plate and Extrapolation ionisation chambers. [19]

Ionisation Chamber	Description
Cylindrical (Farmer type)	<ol style="list-style-type: none"> 1. Measurements in mega-voltage photon radiation therapy. 2. Excellent stability. 3. Small directional dependence. 4. Active volume between 0.1 and 1cm³ with internal length no greater than 25cm and internal diameter no greater than 7mm. 5. Wall material is tissue or air equivalent (low atomic number, Z), with thickness less than 0.1g/cm² and build-up cap thickness of about 0.5g/cm². 6. 1mm diameter aluminium central electrode is used to ensure flat energy dependence.
Parallel-Plate (Attix)	<ol style="list-style-type: none"> 1. Recommended for electron beam dosimetry for energies below 10MeV. 2. Used for surface dose and depth dose measurements in the build-up region. 3. Flat and very thin at 4.8mg/cm² (25microns), with only 2mm separation between the plates. 4. Large guard-ring to reduce over response due to low energy electrons to less than 1%.
Extrapolation	<ol style="list-style-type: none"> 1. Variable volume used for surface dose measurements in orthovoltage and megavoltage x-ray beams and in the dosimetry of beta rays and low energy x-rays. 2. Used in absolute radiation dosimetry when it is directly embedded into a tissue equivalent phantom. 3. Cavity perturbation for electrons can be eliminated by making measurements as a function of the cavity thickness and extrapolating to zero thickness.

Table 3.1: Differences between Ionisation Chambers.

Chapter 4

Method

4.1 Radiation Hardness

The purpose of radiation damage characterization tests is to determine the change of sensitivity of dosimetric devices with accumulated dose. When exposed to ionizing radiation, silicon diodes become subject to radiation damage effects with varying severity reliant on the incident particles used and their energy. These effects act as recombination-generation centres, with equivalent energy levels located in the deep forbidden gap and hence diminish the sensitivity of the detector and reduce the minority carriers lifetime. [56]

Thus as the diffusion length is reduced the sensitive volume of the diode is reduced, and the effect of radiation damage on silicon diodes has been shown to decrease the diode sensitivity. [56] More so there is a specific requirement that medical radiation detectors are to be as stable as possible during their life to avoid frequent and time-consuming recalibration procedures. To circumvent the issue of frequent recalibration and the decreasing sensitivity with accumulated dose the silicon diode would need to be implanted into an epitaxial layer. This reduces the active depth to values that are shorter than the minority carrier diffusion length at the highest operative dose and by defining the planar active area by using a guard-ring structure that is grounded during the operation. Thus when a change in response properties occurs with respect to delivered dose by photon or electron MV energy radiotherapy beams it generally becomes an issue that can be alleviated through pre-irradiation to stabilise the response of the detector.[56]

Radiation damage is a necessary property of a dosimeter to avoid as their performance will be altered with the accumulation of dose. However, if a dosimeter is hardened it will be stable after an initial dose, independent of any further accumulated dose.

To produce a radiation hardened device, several techniques have been introduced in the detector design. These include manufacturing devices on insulating substrates, shielding, choosing substrates with a wide gap for higher tolerance to deep level effects as well as the introduction of bi-polar integrated circuits. [28]

Commercial silicon detectors have a sensitive volume in the region of $1 - 10 \times 10^{-2} \text{cm}^3$, while commercial ionisation chambers have a sensitive volume in the region of $1 \times 10^{-1} \text{mm}^3$. [57]

The measurements for this experiment have all been performed using the Varian Clinac 21Xi Medical Linac at the Illawarra Cancer Care Centre at Wollongong Hospital (NSW, Australia) equipped with a multi-leaf collimator (MLC) Millennium-120 by 6MV photon beams with a flattening filter. The irradiation of the epitaxial diode probes for studying the radiation damage effects on charge collection efficiency of the skin diodes has been performed using a Co-60 source at the Gamma Technology Research Irradiation (GATRI) facility at the Australian Nuclear Science and Technology Organisation (ANSTO, Lucas Heights, NSW, Australia). The effect of radiation damage on the degradation of radiation sensitivity of Epi-1C epitaxial diode is presented in Bruzzi et al. (2007). The passive epitaxial diode is usually less affected by accumulated dose due to the thin sensitive volume and the radiation-generated (RG) centres having a larger capture cross-section for holes than for electrons. Therefore, during radiation exposure, more RG centres are occupied by the minority carriers (holes) in an n-type than in a p-type diode (where the minority carriers are electrons). [16]

To stabilise the response of the skin diodes, they were pre-irradiated with dose increments of 20 kGy up to a total accumulated dose of 80 kGy with response measurements taken at each irradiation step. The response of the skin diodes was measured under standard conditions by delivering 100MU on 6MV linear accelerator photon beam, field size of $10 \times 10 \text{cm}^2$, at depth 1.5 cm in a solid water phantom at a source to surface distance (SSD) of 100 cm. The error bars are calculated as one standard deviation over five repetitions of the same measurement.

4.2 Dose Linearity

The linear response of the detectors are investigated under the standard conditions of a 6MV photon beam with a field size of $10 \times 10 \text{cm}^2$ and a 1.5cm depth in a Virtual Water Phantom (Standard Imaging Inc., Middleton, WI). The response of the diodes are recorded from 50cGy up to 500cGy. The uncertainty is calculated by two standard deviations over three consecutive measurements of each of the three samples from the same production batch and packaged with the same technology.

The investigation proposed by Van Dam et al (2005) and Meyer et al (2001) indicates that as the dose is doubled so is the concentration or response of the detector. Thus the expected signal is said to increase linearly as a function of dose up to 10Gy for commercial semiconductor dosimeters.

4.3 Dose Per Pulse Dependence

The measurement of dose per pulse dependence (DPP) refers to the evaluation of the change of the detector sensitivity due to the change of the instantaneous dose rate in a pulsed radiation beam typical of a medical linear accelerator. [46] It was reported by Rikner and Grusell [46] that n-type silicon diodes are more sensitive to dose per pulse variation than compared to p-type silicon detectors, thus showing an increase in sensitivity with increasing dose per pulse. The reason behind this is that there is a greater reduction in unoccupied radiation-generated centres in an n-type than in a p-type diode, hence allowing for more charge collection and a larger increase in sensitivity with dose rate.

Therefore, an evaluation of the diode characteristics is vital to determine if the technology adopted for the Epi-5B skin diode can be used for quality assurance on a medical linac. The DPP was performed by measuring the diodes and the Attix chambers response placed at a 1.5cm depth and irradiated with a $10 \times 10 \text{cm}^2$ field of 6MV photon beam at 600MU/min within the phantom and varying the SSD from 100cm up to 250cm. The ratio between the charge measured by the silicon diode to the charge measured by the Attix ionisation chamber represents the DPP dependence of the detector which is normalised to the dose per pulse of $2.78 \times 10 \text{cm}^{-4} \text{Gy/pulse}$ corresponding to the SSD of 100cm. This method avoids variation of the spectrum of the radiation and can be used to characterize only the dose rate dependence assuming that the ion chambers dose per pulse dependence is within $\pm 1\%$. [58]

4.4 Percentage Depth Dose

The percentage depth dose (PDD) measurements are obtained for both the silicon epitaxial diode detectors, Epi-5B (n-type) and Epi-1C (p-type), and compared to the Attix ionisation chamber.

The detectors were placed individually in a recess machine of a Virtual Water slab to ensure consistency of the scattering conditions. A 10cm thick slab of $30 \times 30\text{cm}^2$ solid water phantom was used for back-scattering, and several slabs of solid water phantom ranging from 0.1cm to 20cm are used to place on top of the detectors to obtain the depth dose profiles. The detectors were irradiated with 6MV photon beams of 100MU with a $10 \times 10\text{cm}^2$ field size at 100cm SSD for all thicknesses. Thus the SSD is not changing and kept at 100cm in order to accurately measure the PPD for all thicknesses. The results are compared to measurements taken by the Attix ionisation chamber under the same experimental conditions. All the detectors were first pre-irradiated at d_{max} and then normalised to d_{max} .

Additional depth dose profiles were obtained for the skin diode Epi-5B with the epitaxial layer of the skin diode facing downwards. This was conducted under the same experimental conditions as when the diode was facing up as described above to determine whether orientation of the detector affects the PDD results.

Monte Carlo Geant4 version 10.0.p01 [59] simulations were performed to determine the dose distribution at the build-up region generated by the specific linac adopted for this experimental evaluation of the skin diode performances. The incident 6 MV x-ray beam of dimensions $10 \times 10\text{cm}^2$ passing through a $30 \times 30 \times 30\text{cm}^3$ water equivalent block phantom was modelled using Geant4. The source-to-surface distance (SSD) was 100 cm, and the beams were fired from phase space files created from an EGSnrc Monte Carlo based system that models the Varian 2100C Linac at Illawarra Cancer Centre in Wollongong (Australia). The model used to represent the Linac and the phantom setup, along with the physics of transport, has been already validated by experimental results previously. [60] The physics processes modelled in the simulation are from the Geant4 electromagnetic standard physics package and include photoelectric effect, Compton scattering and gamma conversion (photons), ionization, Bremsstrahlung, and positron annihilation (leptons). The particle range cut is set to 0.1mm and the electron/positron maximum step length is 0.1mm. Dose is scored inside the phantom at a voxel size of $0.02 \times 1 \times 1\text{mm}^3$. Each simulation is split into ten parallel jobs each with unique seeds and the mean dose reported. The standard deviation is taken across ten simulations to evaluate uncertainties. In total, 4×10^{13} primary histories are simulated where the primary histories represent the number of electrons hitting the x-ray target in the Linac

head.

The dose uncertainty is approximately $\pm 0.5\%$ of the dose at 1.5cm depth at the beam central axis (CAX) for the $10 \times 10\text{cm}^2$ field size.

4.5 Output Factor and surface field size dependence

The output factor is defined as the ratio of dose per monitor unit at a specific field size to the reference field size.[61]

Output factors are among the clinical beam properties that enter the absorbed dose calculations to a patient on radiation treatment. The procedure in output factor measurements itself is quite simple to follow as it is a point measurement (i.e. one which is done at a point where the detector is static in the medium). The output factors are also quantities that are most problematic to measure in small photon fields since large variations in the measured values are predominant.

The field output factors of high energy x-ray machines describe the relative variation of dose with the size of a beam aperture or field collimation; the larger the field size is the larger the dose at a point in a phantom it becomes. [62] The output factor is defined as the ratio of dose in water, D_w , for a given beam collimator aperture, A , at a reference depth, d , to the dose at the same point and depth, d , for the reference collimator aperture, A_{ref} ,; [62]

$$OutputFactor = \frac{D_w(A, d)}{D_w(A_{ref}, d)} \quad (4.1)$$

For this study the reference field size is $10 \times 10\text{cm}^2$, which is measured at isocentre and at a depth of 10cm (SSD is 90cm), irradiated with 100MU each time. The output factor is measured through placing the pre-irradiated skin diodes (60kGy irradiation dose by Co-60) in the centre of the field for field sizes varying the jaws aperture from $2 \times 2\text{cm}^2$ to $30 \times 30\text{cm}^2$. The alignment of the detector has been performed by maximising the detector response for the $2 \times 2\text{cm}^2$ beam by a scan in the SUP-INF and lateral directions using the couch positioning system (spatial resolution of $\pm 1\text{mm}$). A measurement of the field factor at surface of the phantom has also been performed to evaluate the capabilities of the detector to measure surface dose as a function of the field size defined by the jaws. The silicon epitaxial diodes are benchmarked using Gafchromic EBT3 film, the Attix ionisation chamber and the

MOSkin, frequently used for interface measurements and described in several works. [48][63][64]

The films were calibrated using $1.5 \times 1.5\text{cm}^2$ cuts and scanned using a flatbed scanner (Epson 10000XL scanner; Epson America, Inc. Long Beach, CA) 24 hours after irradiation to allow for post-irradiation development. The films were scanned in transmission mode, at a resolution of 72 dpi and 48 bit RGB data format. Analysis of three scanning repetition for each film placed with the same orientation have been performed using ImageJ 1.46r software (National Institute of Health, Bethesda, MD) and one standard deviation of the optical density used as uncertainty. A template was used to scan the films at the centre of the scanner bed to avoid non-uniformity associated with the position of the film in respect to the scanner lamp or sensor. Only the red channel was used for analysis of a region of interest (ROI) at the centre of the film. The films used to perform the measurements have been pre-scanned for evaluation of the background optical density and to take care of the non-uniformities associated with the specific film cut. Butson et al. provides in depth details of the preparation and scanning procedure adopted for the analysis of the EBT3 film.

As a result of the small field dosimetry for both the p- and n-type silicon diode detectors, a severe over-response can affect the outcome due to the lack of lateral charged particle equilibrium.[61] This occurs when the beam source radius becomes small in comparison to the maximum range of secondary electrons. Thus, resulting in disequilibrium which renders the assumptions of the Bragg-Gray cavity theory ineffective. There is also an underestimation of dose when the field sizes are small due to the heightened sensitivity of the silicon diode detectors to scattered radiation (2% for $2 \times 2\text{cm}^2$ field size).[65]

4.6 Angular dependence

The angular dependence of the n-type skin diode (Epi-5B) response was measured experimentally to determine whether angular positions of the linac affects the result and function of the detector. This characteristic is of high importance when performing off-axis measurements. It has been suggested by Shi et al. (2003) that the more “oblique” the radiation, i.e. the larger the angle between the beam axis and the diode symmetry axis, the angular dependence becomes higher, which may amount to more than 5% for angles of 60 degrees and greater. [25]

The angular dependence obtained for the response of the Epi-5B detector was evaluated under two different conditions. The first condition being that the Epi-5B detector was placed in a cylindrical PMMA phantom at 15cm depth (aligned

with the central axis of the phantom) and placed at isocentre with a field size of $10 \times 10\text{cm}^2$ of a 6MV photon beam. The response of this detector was normalised to 0 degrees corresponding to the beam perpendicular to the detectors face-up configuration.

The second condition corresponds to the detector being placed at surface of a $30 \times 30\text{cm}^2$ Virtual Water Phantom with 10cm of backscattering. This configuration benchmarked the Epi-5B detector to the Attix ionisation chamber, after correction of its intrinsic angular dependence, using a field size of $10 \times 10\text{cm}^2$ at 100cm SSD for a 6MV photon beam.

For both conditions 100MU was delivered for each gantry angle position rotating from -60 degrees to +60 degrees in 15 degree increments and responses normalised to the 0-degree gantry position.

Chapter 5

Results and Discussion

5.1 Radiation Hardness

The skin diode (Epi-5B) is fabricated on a $10\Omega\text{-cm}$ n-type silicon substrate which is potentially sub-optimal for radiation detectors exposed to high energy photon radiation for extended periods. The radiation damage associated with therapy photon beams is mainly from the recoil energy of secondary electrons. The radiation damage with electron beams is due to the energy transfer by of primary and scattered electrons to the silicon crystal lattice. The use of the detector in passive mode mitigates the problem associated with the leakage current increase. This increase is due to the accumulation of generation and recombination centres in the silicon substrate and the trapped charge at the silicon-silicon oxide interfaces. The residual radiation damage effect is the variation of the detector response as a function of the accumulated dose.

Figure 5.1 demonstrates the variation of the response of the n-type silicon skin diode detector (Epi-5B) as a function of the dose accumulated from the Co-60 gamma source. As expected there is a response decrease with accumulated dose. However, the response becomes stable with a variation of approximately $-0.05\%/kGy$ after $60kGy$. The response decreases by a factor of 25% in the first $20kGy$ of accumulated dose due to the reduction of the carrier lifetime and shrinking of the diffusion length. This result mainly affects the charge generated around the P+ junction coming from lateral directions. As soon as the diffusion length is shorter than $30\text{-}50\mu m$, the collection of the charge stabilises, making the detector response variation within 2%. The result is in agreement with previous results on thinned and epitaxial silicon detector studies on a substrate with similar resistivity by Bruzzi et al. (2007) and Petasecca et al. (2007). Also consistent with data mentioned by Larin et al. (1968),

Rikner and Grusell (1983) and Van Dam et al. (1990) as that there is a loss in sensitivity as a function of the dose which accumulates over the diode detectors lifetime.

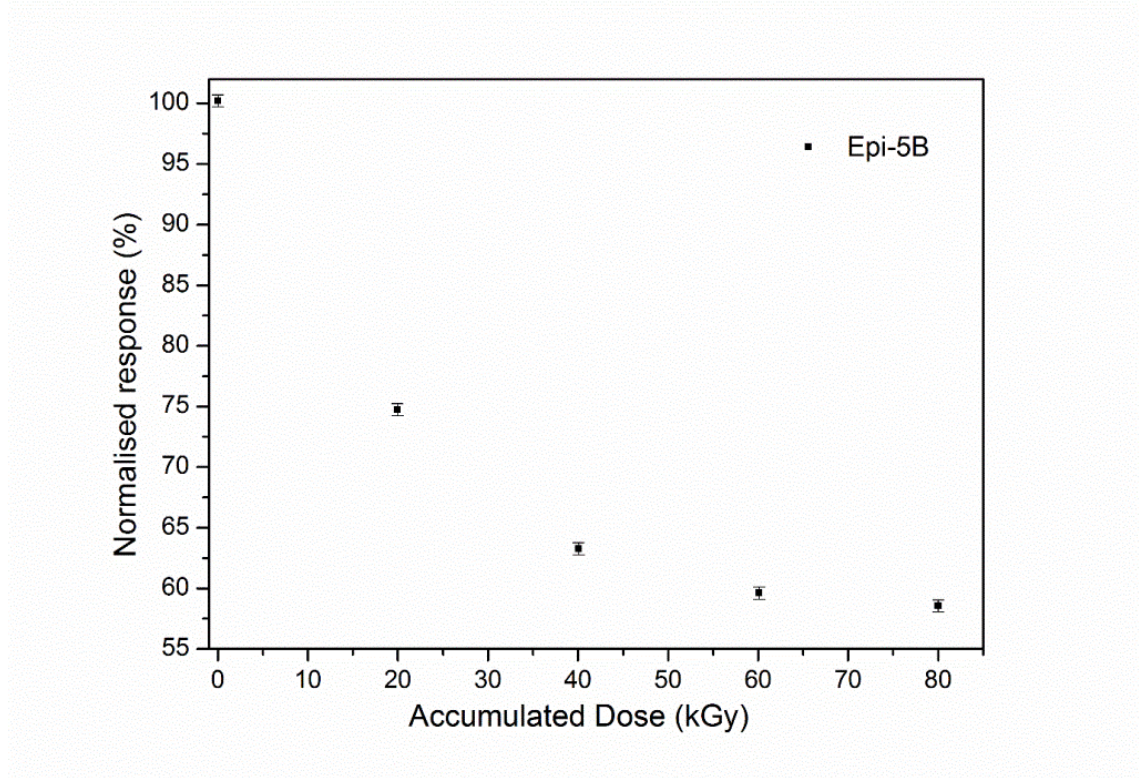


Figure 5.1: Response variation of the skin diode (Epi-5B) as a function of accumulated dose from a Co-60 gamma source.

5.2 Dose Linearity

Figure 5.2 presents the dose linearity for the accumulated dose varying from 50cGy to 500cGy for Epi-5B and Epi-1C epitaxial diodes after pre-irradiation by 60kGy, respectively. Both these diodes display a linear relationship between the dose and detector response over a 500MU range, which is an expected characteristic when using diode detectors.

Table 5.1 summarises the dose calibration factors from charge to dose extracted from the linearity measurements. The conversion factor demonstrates that despite the sensitivity of Epi-5B it is very low in comparison with the thicker epitaxial diode Epi-1C, its reproducibility is still within 0.2% with excellent linearity ($R^2=1$ for Epi-5B). The reproducibility of the diode detectors is determined based on two standard deviations of five repeated measurements of each accumulated dose.

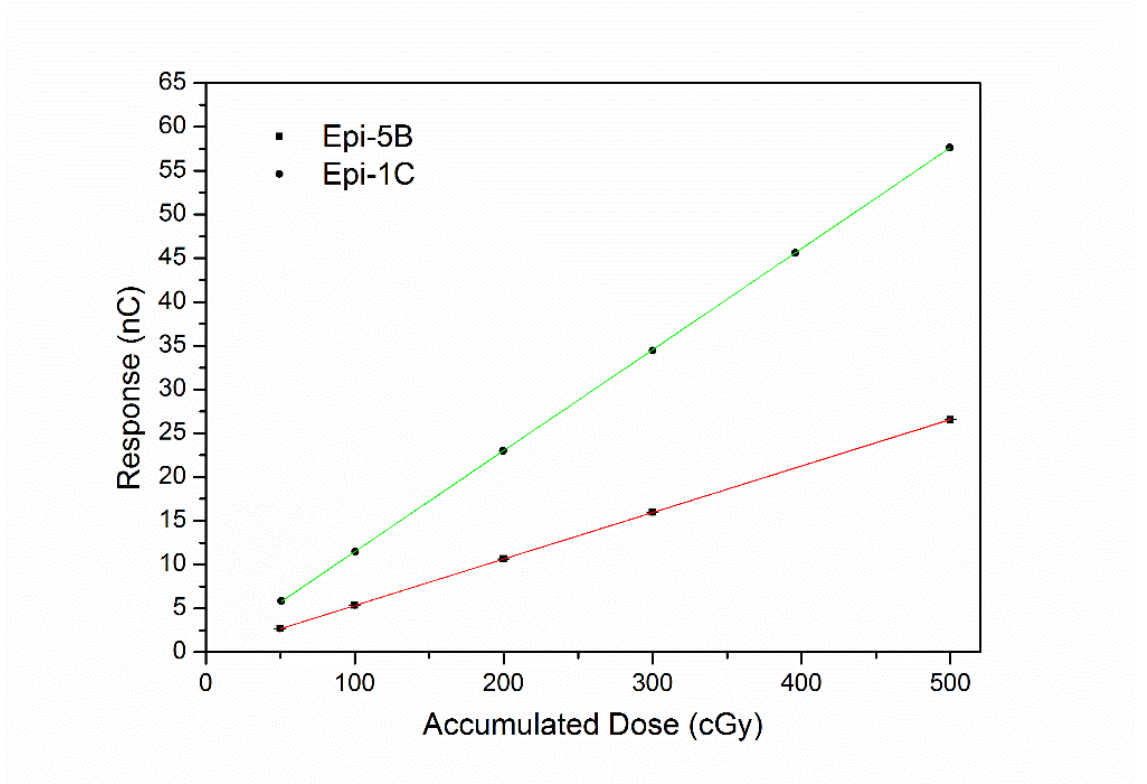


Figure 5.2: Dose linearity response for the Epi-5B (squared symbol) and Epi-1C (dotted symbol) epitaxial silicon diodes.

Diodes	R ²	Response (pC/cGy)
Epi-1C	0.9999	115.18 ± 0.14
Epi-5B	1.000	53.12 ± 0.03

Table 5.1: Dose calibration factors of the Epi-5B and Epi-1C.

5.3 Dose per pulse dependence

Figure 5.3 demonstrates the dose per pulse dependence (DPP) response of the 5B n-type epitaxial detector. The response is normalised to the dose measured by the ion chamber from a 6MV photon beam at $2.78 \times 10\text{cm}^{-4}\text{Gy/pulse}$ and at 1.5cm depth in solid water with a beam field size of $10 \times 10\text{cm}^2$ and 100cm SSD. Dose rate dependence in silicon diodes can potentially affect the capability of the detector to reconstruct accurately dose profiles and depth dose distributions. The skin diode shows a variation of less than 5% within the range between 10^{-4} and $2.78 \times 10\text{cm}^{-4}\text{Gy/pulse}$. The percentage depth dose measurements present a $\pm 1\%$ agreement compared to the parallel plate ion chamber.

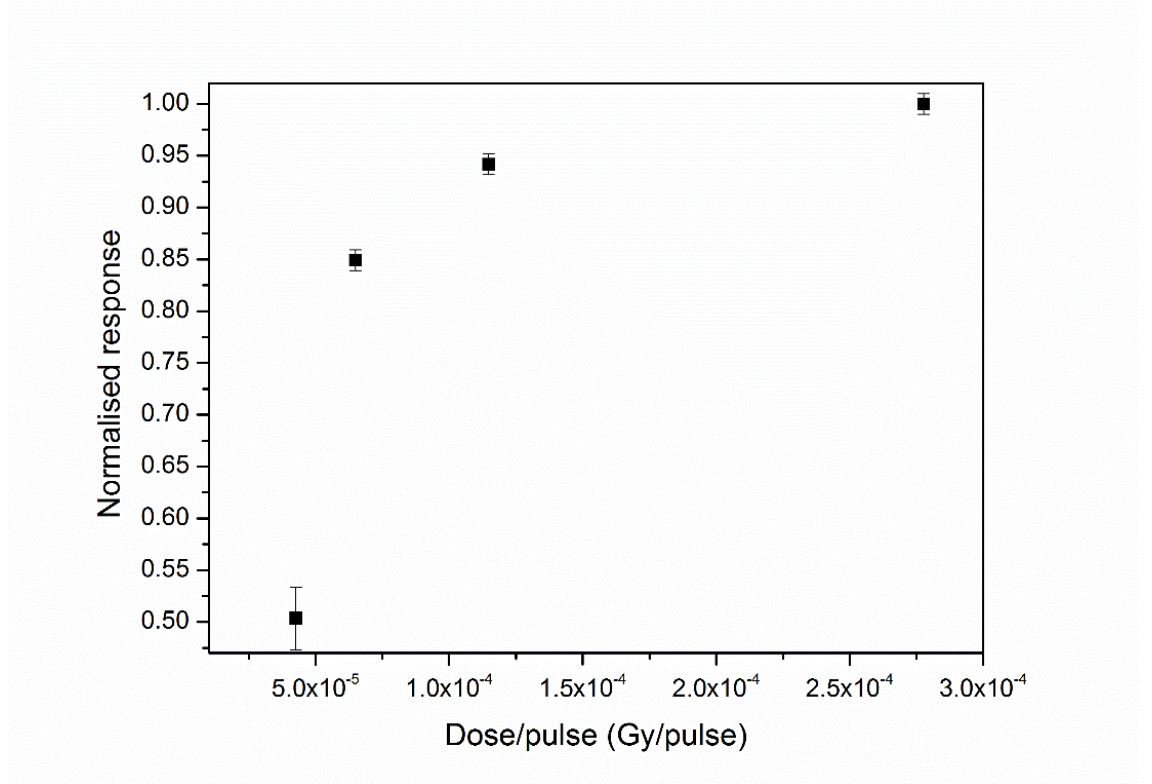


Figure 5.3: Dose per pulse (DPP) response of the skin diode Epi-5B estimated at D_{max} (1.5cm) in solid water with a 6MV photon beam of $10 \times 10 \text{ cm}^2$ field size varying SSD from 100cm to 250cm.

The epidiode 5B detector exhibited an increase in response as the dose rate (Gy/pulse) increased. This is explained by the Shockley-Read-Hall (SRH) recombination model which is the recombination and generation of holes and electrons in semiconductors that occur through the mechanism of trapping.[16]

More so, as the instantaneous dose-rate increases, due to treating a short SSD, the rate of minority carrier generation also increases. Thus, if the recombination-generation centre concentration is insufficient, then the diode sensitivity also increases as a larger fraction of the charge produced by the radiation. The charge is then available to be collected by the electrometer. For linacs, dose is delivered in pulses of approximately 100 pulses/second of width approximately $2\text{-}6\mu\text{s}$ and the instantaneous dose rate within a single radiation pulse determine the rate of charge generation. This is shown in Figure 5.3

AAPM RPT 87 states that all diode detectors exhibit a change in sensitivity with SSD and that the changes in SSD will change the instantaneous dose rate, thus changing the probability of indirect recombination. [16] It is also important to note that the average dose rate, which is nominally 100-600cGy/min is not the same as the instantaneous dose rate in an accelerator pulse which is 103-104cGy/min. [16] This dose rate is 102-103 times higher than the average rate because the charge

collection time of the diode and electrometer is typically much shorter than the time between the pulses. In addition, the response of an in vivo dosimetry system is not expected to depend upon the average dose rate.

During the irradiation of diode detectors, electron-hole pairs are produced at a rate that increases as a function of dose-rate (dose per unit time). When the dose-rate is high as is the case for pulse radiation produced by linear accelerators, pile up occurs. This phenomenon arises when the ions are produced at such a high rate that the recombination cannot continue and more charge carriers escape recombination than at lower dose-rates. Therefore, diode sensitivity decreases when decreasing the dose per radiation pulse. This has been observed for both n- and p-type detectors (Grusell and Rikner, 1983).

In relation to the dose per pulse test, as the SSD increases, the sensitivity of the detector decreases by 50% for a 10-fold increase in dose rate (Gy/pulse) reduction thus altering the probability of indirect recombination.

5.4 Percentage Depth Dose

Figure 5.4 presents a comparison of the percentage depth dose (PDD) measurements from surface to 20cm depth in Virtual Water with the skin diode and the Attix ionisation chamber. The results are normalised to d_{max} for a 6MV photon beam with $10 \times 10 \text{cm}^2$ radiation field area. The observed maximum difference between the PDD measured with the skin diode and calculated with Geant4, excluding the outsider point at 1cm depth, is within $\pm 2\%$ with an agreement within $+0.5\%$ at a water equivalent depth of 0.07mm. The difference between skin diode and the uncorrected Attix chamber at 0.07mm depth is approximately $+2\%$. This difference reduces to 0.2% if the ion chamber response is corrected for skin dosimetry as suggested by Gerbi and Khan implying an effective depth of measurement for the un-corrected Attix chamber of approximately $30\mu\text{m}$. [54][33]

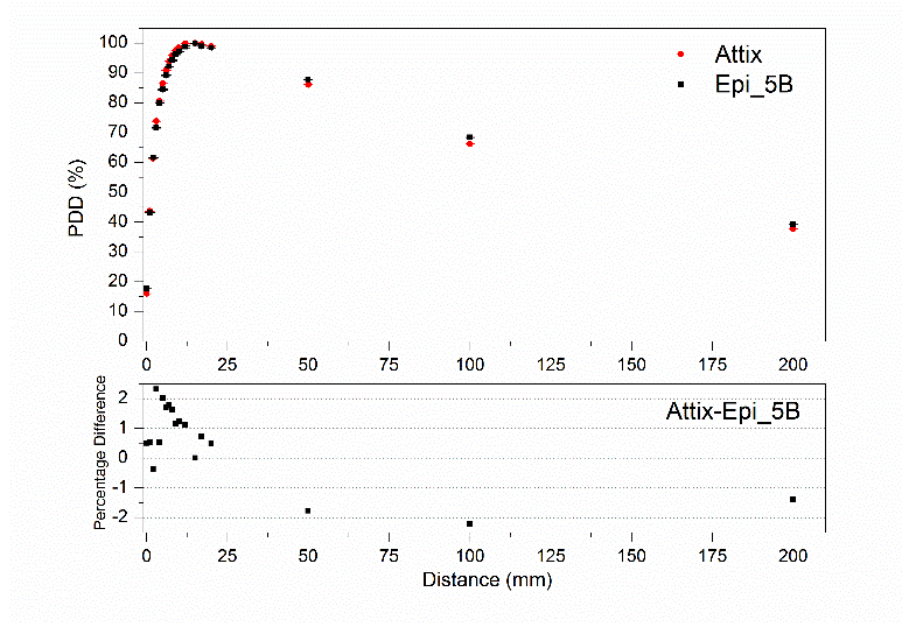


Figure 5.4: Percentage Depth Dose measured by the skin diode in comparison to the Attix ionisation chamber with no build up cap and no correction factors applied.

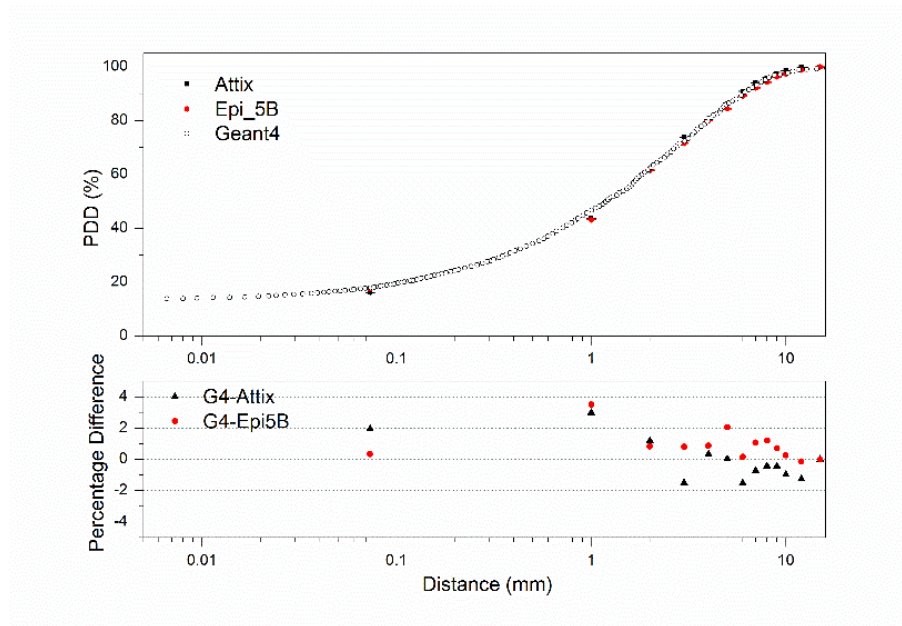


Figure 5.5: Comparison of the same data set measured with Attix and Epi-5B with the simulations performed by the means of Geant4 in water and represented in logarithmic scale of the depth in water.

Figure 5.6 displays the comparison of the PDD measured in standard conditions between the thick epitaxial Epi-1C diode and the Attix ionisation chamber in Virtual Water. The observed maximum difference between the PDD measurements is +5.5% representing an over-response of the epitaxial Epi-1C diode on a surface of the phantom; while its agreement with the Attix ionisation chamber at depths greater than 5mm is less than 1.5%.

This measurement has been performed to determine the sensitivity of the WED of dose measurements to the thickness of the epitaxial layer for the fabrication of an effective skin dosimeter with WED of dose measurement 0.07mm when placed on a surface of the phantom, even if the diode utilizes the same “drop in” packaging technology. Another example of the accuracy required for the design of a skin dosimeter using silicon is shown in Figure 5.7, where the skin diode has been irradiated face-down. Compared to the Attix ionization chamber, the face-down Epi-5B over-responses has +20% more dose recorded at the surface.

In the face-down configuration, the diode substrate is irradiated before reaching the sensitive volume. The different WED corresponding to this configuration generates a discrepancy in surface dose measurements of approximately +20%. This is expected and can be observed in Figure 5.7 as the 400 μ m silicon above the sensitive volume generates a build-up with WED of approximately of 1mm. This increased detector response is due to the dose enhancement effect of the high Z of silicon, i.e. additional number of electrons are forward scattered from the silicon substrate to the sensitive volume of the epitaxial layer downstream. Thus, with decreasing photon energies, this effect is gradually reduced as the competing effect of the x-ray attenuation due to the 0.400mm silicon substrate.

The n-type and p-type epitaxial silicon diode detectors present a $\pm 1\%$ agreement of the measured PDD compared to the parallel plate Attix Ionisation Chamber downstream of d_{max} regardless of the substrate size. The thin substrate detector used (n-type, 5B with 7 μ m substrate) shows an agreement with the Attix ionisation chamber response at the surface within +1.7%. The thick substrate detector used (p-type, 1C with 50 μ m substrate) demonstrates a large discrepancy up to +7% at the surface. This effect can be related to the excess of charge contribution due to the backscattering from silicon in thick devices which becomes predominant at low depths due to the lack of charge particle equilibrium. More so when the orientation of the detector is reversed for the epidiode 5B detector a discrepancy of +20% at the surface compared with the Attix ionisation chamber is measured for the PDD. However, downstream of d_{max} for this detector configuration, there is a 1.5% discrepancy and 400 μ m silicon above the sensitive volume will generate a large build-up thus indicating that orientation impacts the results when using a silicon detector

diode for skin dosimetry.

The Geant4 simulations of the percentage depth dose in the build-up region have been used to derive the effective WED of 0.07mm and 0.03mm of the skin diode and the Attix ionisation chamber, respectively. The thickness of the sensitive volume of the detector in steep dose gradients is a major factor for accuracy in skin dosimetry at a water depth of 0.07mm. The Epi-1C detector with 50 μ m thick epitaxial layer was found to have a WED of 1mm, making this diode unsatisfactory for skin dosimetry. While the Epi-5B detector with a 7 μ m thick epitaxial layer produced a WED of approximately 0.075mm, indicating that this diode is ideal for skin dosimetry.

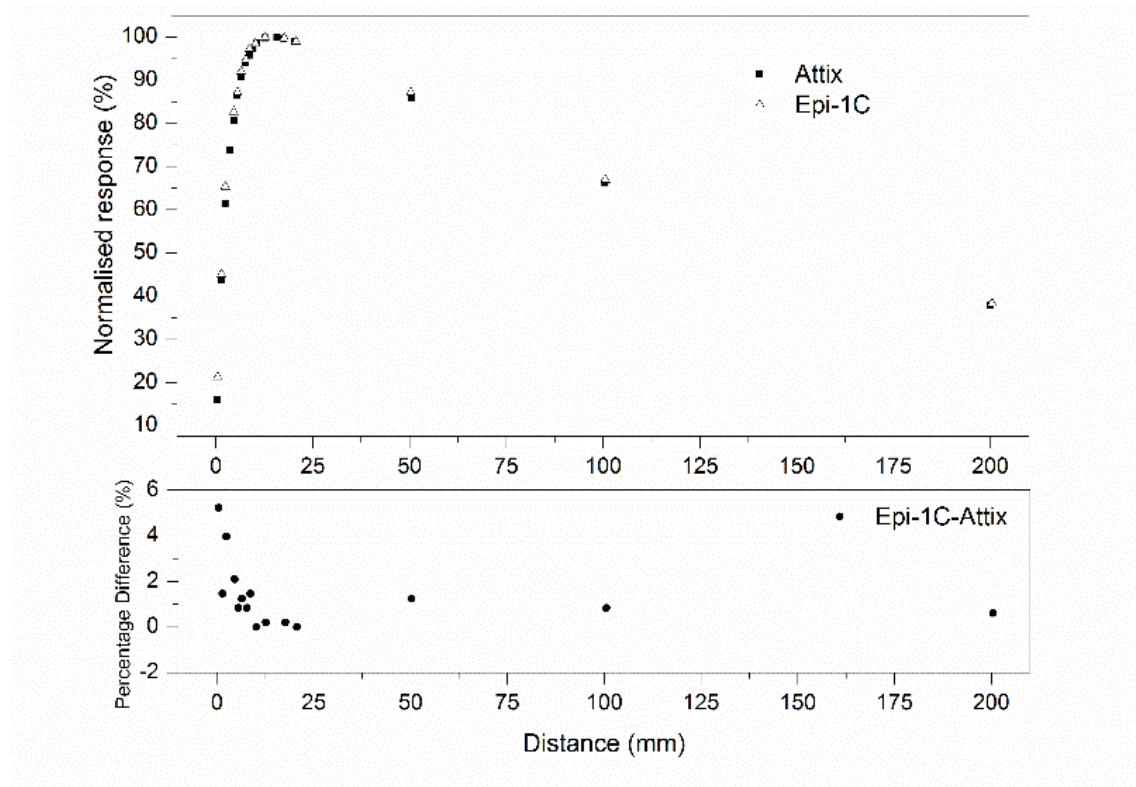


Figure 5.6: PDD measured by Epi-1C in comparison to Attix IC in a solid water phantom Epi-1C is “face up”.

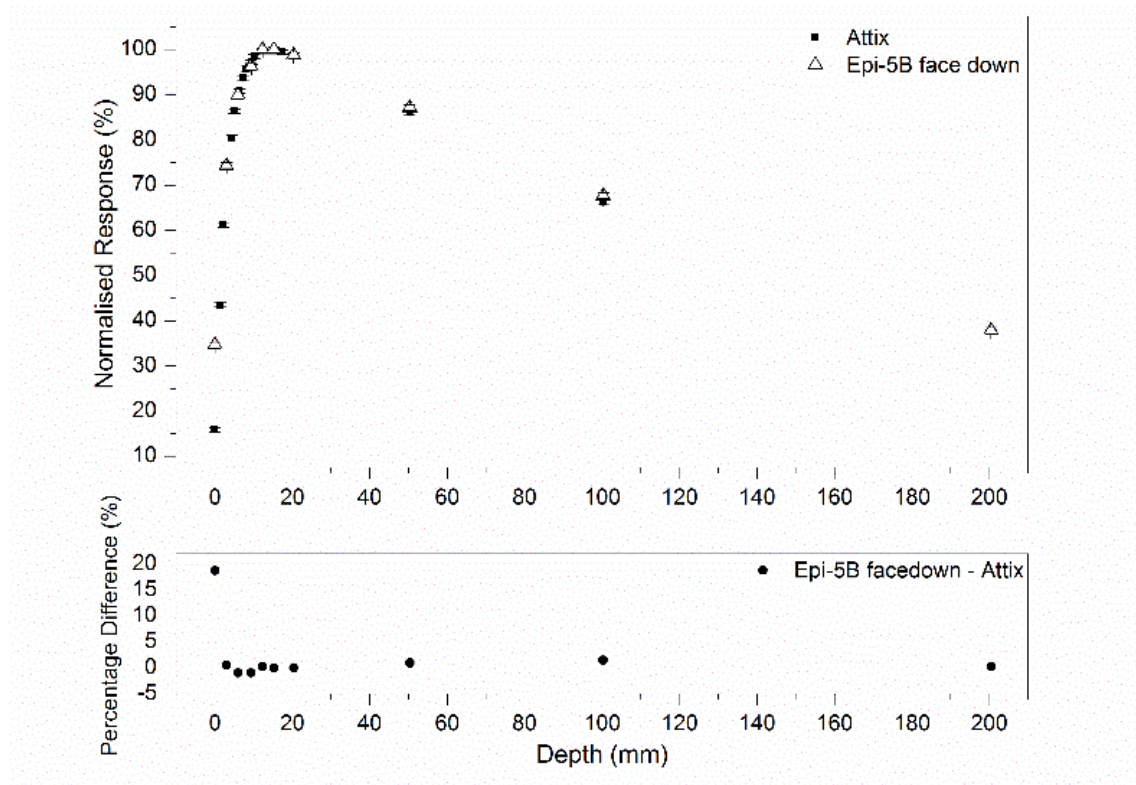


Figure 5.7: PDD measured by Epi-1C in comparison to Attix IC in a solid water phantom Epi-5B is “face-down”.

5.5 Output Factor and surface field size dependence

Output factor is known as a function of the field size due to the factor that as the field size increases, not only will the primary radiation increase however the number of scattered radiation also increases. This results in a higher rate of ionization and therefore a higher dose measured by the detectors. This is shown in Figures 5.8 and 5.9, which are normalised to the reference field size $10 \times 10 \text{ cm}^2$.

Figure 5.8 displays the output factor measured by the skin diode and compared to EBT3 film and MOSkin detector at 10cm depth within the Virtual Water phantom. As expected, MOSkin and EBT3 film agree within 1.2% from a square field size (SFS) of 0.5cm up to 30 cm proving the quality of the experimental setup which confirms results obtained previously for small field dosimetry studies. [66]

The skin diode in the face-up configuration has been tested from an SFS of 2cm up to 30cm with an agreement within 2% in respect to EBT3 film. The lack of data below an SFS of 2cm is due to the very poor signal to noise ratio of the detector in small field sizes at a depth of 10cm in the solid water phantom.

Figure 5.9 shows the measurement of the surface field size dependence using the Attix ionisation chamber and the skin diode normalised to a field size of $10 \times 10\text{cm}^2$ using different Kapton build-up layers. The configuration with 0.05mm of build-up matches the skin diode response within 3% for all the field sizes investigated.

More so the response of the Epi-5B detector in a virtual water phantom is determined by the secondary electrons. In the free air geometry, the diode response is determined by photons, i.e. the mass energy absorption coefficients of the silicon. [48]

Skin dose increases as a function of the field size and depends on the WED measurement. The skin diode and the Attix ICs response with field size are different due to the fact that the WED of the IC is about 0.025mm [33], in contrast to the WED of the skin diode, estimated to be approximately 0.075mm. Adding two Kapton sheets of $25\mu\text{m}$ thick, and matching field size response of the response of the ionisation chamber to the skin diode confirms that the skin diode WED is approximately between 0.07 and 0.08mm, as estimated by the Geant4 simulations. Thus due to the small sensitive volume of the Epi-5B detector, it is advantageous for small field surface dosimetry compared to Attix ionisation chamber.

The use of the skin diode for low dose rate measurements is challenging due to the trade-off between a thin sensitive volume and the signal-to-noise ratio. This was observed during output factor measurements, where measurements in fields below $2 \times 2\text{cm}^2$ were impossible with the electrometer adopted. Adapting a larger area for the p+ top junction without enlarging the overall diode size by reducing the external guard-ring would double the sensitivity of the sensor solving the issue of the signal-to-noise ratio. This would increase the amount of charged collected without perturbing the beam with a larger silicon die.

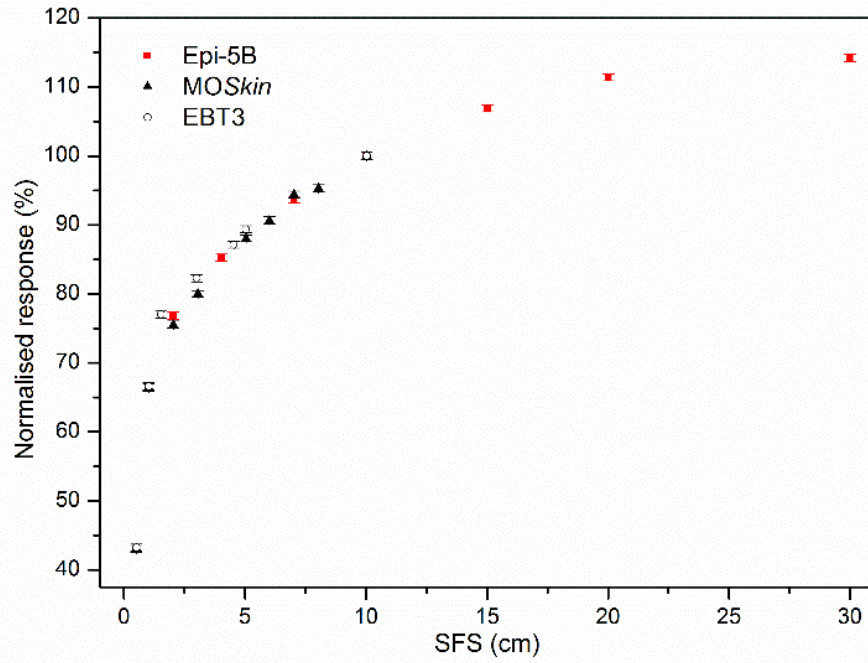


Figure 5.8: Output factor measured by MOSkin, EBT3 film and skin diode Epi-5B at 10cm depth in Virtual Water phantom.

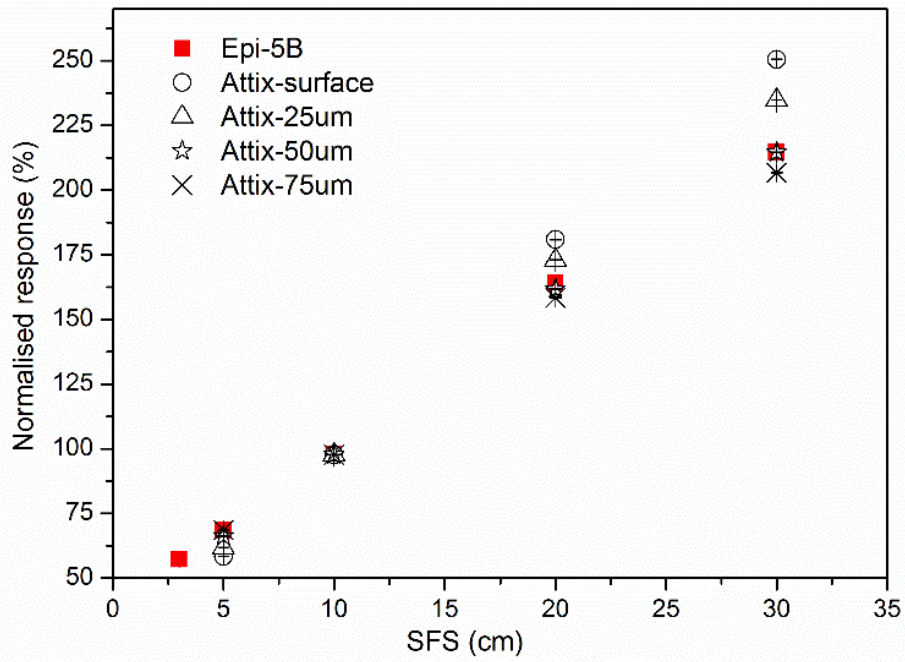


Figure 5.9: Field size dependence of the skin diode placed at surface of the phantom in comparison with Attix with different build up thickness.

5.6 Angular dependence

The angular dependence response of the epitaxial silicon diode detector was studied in the context of in vivo skin dose measurements. For surface dose measurements, where CPE does not exist, it is important to note that the surface dose increases with the beam incidence angle. Correct measurements of the skin dose at different angles of beam incidence are valuable for both treatment planning system (TPS) verification [13] and for studies correlating acute skin toxicity to dose delivered to the skin in head and neck or breast cancer treatments.

The epitaxial 5B detector is a planar silicon device which suffers of an intrinsic angular dependence. In order to accurately estimate the effect of skin dose deposition from tangential beams, we must compensate for the intrinsic angular dependence of the device. This can be achieved by testing the detector placed in the central axis of a cylindrical PMMA phantom of radius 15cm and aligned with the linacs isocenter.

Figure 5.10 shows the result for the intrinsic angular dependence of the Epi-5B normalised to the response of the detector at gantry angle 0-degree (beam incident orthogonally). As expected, the device behaves similarly to a planar device with a very thin sensitive volume: the largest variation (-8%) occurs at 90 degrees and the attenuation of the beam incident from the back-side of the detector is approximately -2%. The correction factor for a tangential beam with angle of $\pm 60^\circ$ as expected in a 3D conformal treatment of breast cancer will be +5% at largest.

To evaluate the ability of the skin diode to measure skin dose at various beam incidence angles, 100MU of a 6MV photon beam with a $10 \times 10\text{cm}^2$ field size is delivered with the gantry position rotated from -60degrees to +60degrees with 15 degree increments. The skin diode and the EBT3 film are placed on a surface of the phantom and their readings are normalised to the reading obtained at 0 degree gantry angle with a fixed SSD of 100cm.

Figure 5.11 shows a comparison between the angular dependence response of the skin diode (corrected for its intrinsic angular dependence), the film and the Attix ionising chamber. As the beam incidence angle increases, the measured surface dose increases as well, due to d_{max} being shifted towards the surface.

The skin diode with a 0.005mm epitaxial layer is suitable for skin dosimetry with a WED of 0.075mm. The angular response at the surface of the phantom agrees within 3% of relative variation between the skin diode and EBT3 film with beam incident angles in the range between $\pm 60^\circ$. The skin diode shows a minimal angular dependence comparable with the film response, however it also measures the

dose at the WED of 0.07mm which cannot be achieved by film. Film has a WED of dose measurement at approximately 0.1mm due to the polyamide protection layer above the radiation sensitive polymeric substrate (0.05mm thick) [13][67]. The Attix IC response shows a large over-response up to +20% at ± 60 degree as confirmed by other studies. [5]

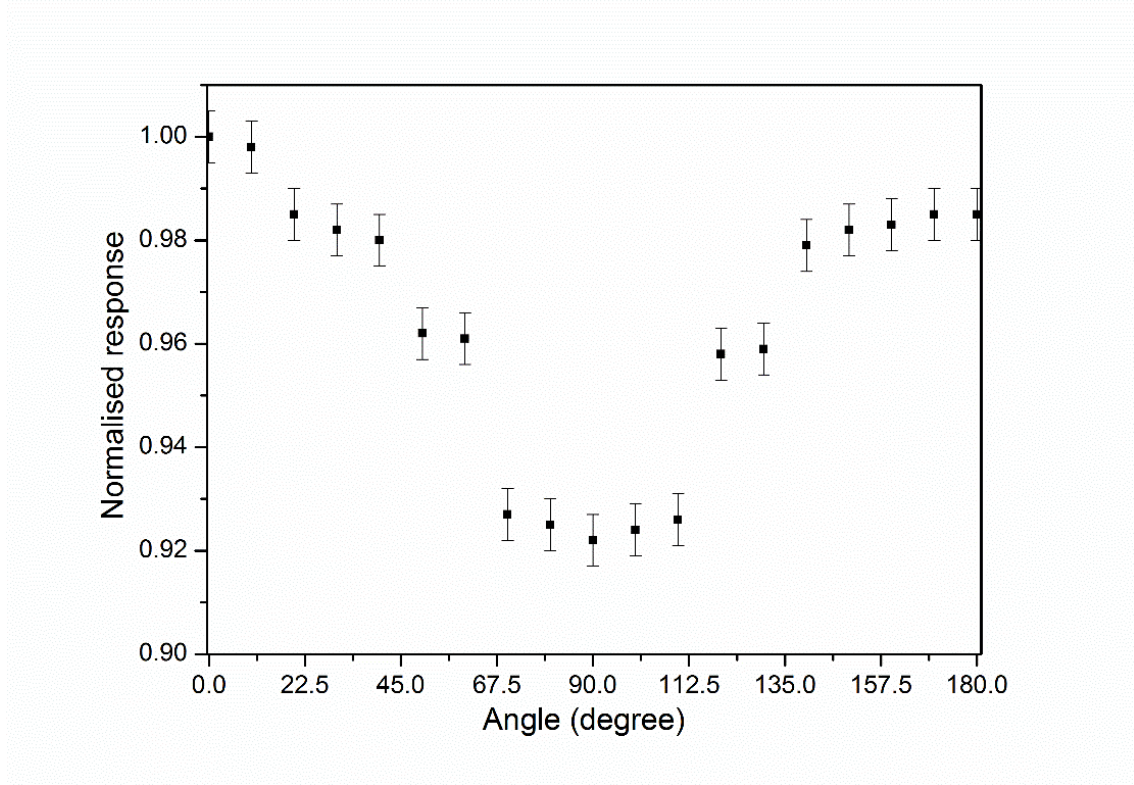


Figure 5.10: Normalised intrinsic angular response of the skin diode placed in centre of a cylindrical PMMA phantom of radius of 15cm as a function of the angle. Center of the phantom is placed in isocentre. Normal incident angle is 0 degree.

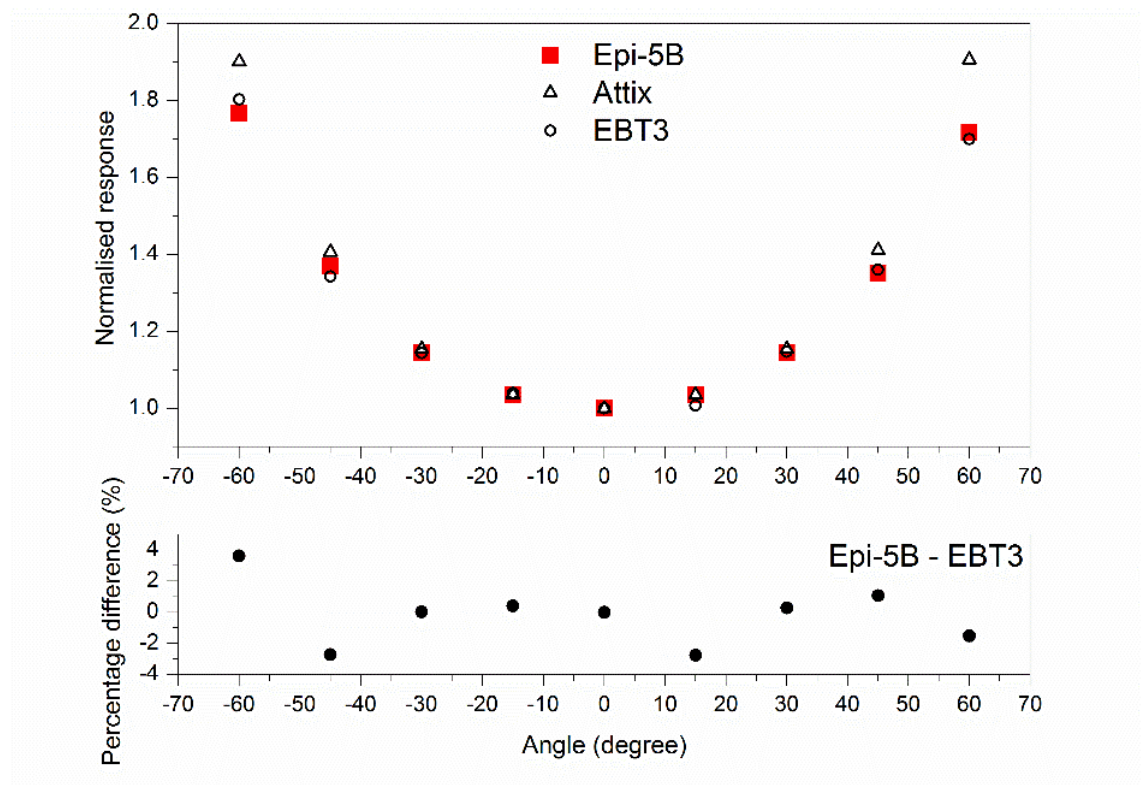


Figure 5.11: Comparison of the normalized surface dose angular dependence measured by the skin diode, EBT3 film and Attix chamber at surface of a Virtual Water phantom for a 6MV photon beam.

Chapter 6

Conclusion and Future Work

Silicon diode detectors with different substrate thicknesses $50\mu\text{m}$ known as 1C and $7\mu\text{m}$ known as 5B are compared with the Attix parallel plate ionisation chamber for different field sizes, percentage depth doses, angles, dose rate dependence and radiation hardness to determine which detector is ideal for in vivo skin dosimetry. An ideal in vivo dosimeter should have the following characteristics: (i) thin enough to determine dose delivered to shallow depths; (ii) reproducibility of WED (water equivalent depth) (packaging); (iii) wide dynamic range; (iv) linear in dose response; (v) insensitive to dose rate variations; (vi) energy and temperature independent; and (vii) able to provide real-time dosimetric information.[13]

This work presents a feasibility study towards the development of a silicon diode that can measure the skin dose accurately in respect to clinical standards for QA of medical linacs. The use of a diode for skin dose measurements is of interest due to the possibility of developing an array of such detectors for real time, in-vivo skin dose mapping in several radiotherapy and diagnostic imaging modalities, where the risk of acute skin toxicity is a serious issue for the patients quality of life. The skin diode is fabricated on a 0.005mm thick epitaxial silicon layer placed above 0.4mm thick silicon substrate and embedded in a thin water equivalent package using “drop in” packaging technology. The skin diode has a WED of $0.075 \pm 0.005\text{ mm}$, as recommended by the ICRP and can be used to measure the skin dose delivered by oblique radiation beams.

The skin diode can also be used for conventional QA dosimetry in radiation therapy because it has a linear dose-response over a dynamic range from 25 to 500 cGy and minimal intrinsic angular dependence, in conjunction with the ability to measure the PDD within 2% compared to ionisation chamber.

The challenge to be addressed is the improvement of signal-to-noise ratio for low dose rate applications, which could be achieved by increasing the sensitive area of the skin diode and electrometer sensitivity. Such a device would be suitable as a multi-purpose diode for real-time QA measurements in radiation therapy.

Bibliography

- [1] Wolmark N, Fisher B, Anderson S, Bryant J, Margolese RG, Deutsch M, Fisher ER, Jeong JH. “Twenty-year follow-up of a Randomized Trial comparing Total Mastectomy, Lumpectomy, and Lumpectomy plus irradiation for the treatment of invasive Breast Cancer”. In: *N Engl J Med*. 347.16 (2002), pp. 1233–1241.
- [2] S. Darby et al. “Effect of radiotherapy after breast-conserving surgery on 10-year recurrence and 15-year breast cancer death: Meta-analysis of individual patient data for 10 801 women in 17 randomised trials”. In: *The Lancet* 378.9804 (2011), pp. 1707–1716.
- [3] ICRP (International Commission on Radiological Protection). *The Biological Basis For Dose Limitation In The Skin*. Vol. 22. 2. 1992.
- [4] D.E Mellenberg. “Determination of build-up region over-response corrections for a Markus-type chamber”. In: *Medical Physics* 17.6 (1990), pp. 1041–1044.
- [5] Gad Shani. *Radiation Dosimetry Instrumentation and Methods*. CRC Press LLC Washington DC, 2001, pp. 121–122.
- [6] Bo Nilsson and Anders Montelius. “Fluence perturbation in photon beams under nonequilibrium conditions”. In: *Medical Physics* 13.2 (1986), pp. 191–195.
- [7] T Kawachi, H Saitoh, and Inoue. “Reference dosimetry condition and beam quality correction factor for CyberKnife beam”. In: *Medical Physics* 35.10 (2008), pp. 4591–4598.
- [8] Nicholas Hardcastle et al. “Dosimetric verification of helical tomotherapy for total scalp irradiation”. In: *Medical Physics* 35.11 (2008), pp. 5061–5068.
- [9] Martin J Butson, Tsang Cheung, and P K N Yu. “Scanning orientation effects on Gafchromic EBT film dosimetry.” In: *Australasian Physical & Engineering Sciences in Medicine* 29.3 (2006), pp. 281–284.
- [10] Ben Mijnheer et al. “In vivo dosimetry in external beam radiotherapy.” In: *Medical Physics* 40.7 (2013), p. 070903.
- [11] V. C. Colussi et al. “In vivo dosimetry using a single diode for megavoltage photon beam radiotherapy: implementation and response characterization.”

- In: *Journal of applied clinical medical physics / American College of Medical Physics* 2.4 (2001), pp. 210–218.
- [12] A.H Zhuang and A.J Olch. “Validation of OSLD and a treatment planning system for surface dose determination in IMRT treatments”. In: *Medical Physics* 41.8 (2014).
 - [13] Wei Loong Jong et al. “Characterization of MOSkin detector for in vivo skin dose measurement during megavoltage radiotherapy”. In: *Journal of Applied Clinical Medical Physics* 15.5 (2014), pp. 120–132.
 - [14] I.S Kwan et al. “Skin dosimetry with new MOSFET detectors”. In: *Radiation Measurements* 43.2-6 (2008), pp. 929–932.
 - [15] Paul A. Jursinic. “Angular dependence of dose sensitivity of surface diodes”. In: *Medical Physics* 36.6 (2009), pp. 2165–2171.
 - [16] AAPM N87. *Diode in vivo dosimetry for patients receiving external beam radiation therapy*. Tech. rep. 87. 2005, pp. 1–64.
 - [17] Frank Herbet Attix. “Introduction to Radiological Physics and Radiation Dosimetry”. In: *Wiley-VCH*. 2004, p. 264.
 - [18] Tatsiana A. Reynolds and Patrick Higgins. “Surface dose measurements with commonly used detectors: A consistent thickness correction method”. In: *Journal of Applied Clinical Medical Physics* 16.5 (2015), pp. 358–366.
 - [19] E.B Podgorsak. “Radiation Oncology Physics: A Handbook for Teachers and Students”. In: *British journal of cancer*. Vol. 98. 2008, p. 1020.
 - [20] ICRP (International Commission on Radiological Protection. “The 2007 Recommendations of the International Commission on Radiological Protection”. In: *ICRP Publication 103* 37.2-4 (2007), pp. 1–332.
 - [21] Jeremy Jone. *Equivalent Dose*. 2016. URL: <https://radiopaedia.org/articles/equivalent-dose>.
 - [22] Claire Cousins and Christopher Clement. “International commission on radiological protection”. In: *Annals of the ICRP* 1.12 (2011), pp. 1–12.
 - [23] N Jornet et al. “Comparison study of MOSFET detectors and diodes for entrance in vivo dosimetry in 18 MV x-ray beams.” In: *Medical physics* 31.9 (2004), pp. 2534–42.
 - [24] Huda Hassan Mahgoub Mohammed. “Clinical application of in vivo dosimetry for external telecobalt machine”. In: January (2011).
 - [25] Jan Van Dam and Ginette Marinello. “Methods for in vivo dosimetry in external radiotherapy”. PhD thesis. 2006.
 - [26] David Zahra. “MOSFET dosimetry: MOSkin dosimetric characteristics in a 6MV x-ray beam”. In: *University of Wollongong Thesis Collection* (2009).

- [27] Indra J. Das et al. “Accelerator beam data commissioning equipment and procedures: Report of the TG-106 of the Therapy Physics Committee of the AAPM”. In: *Medical Physics* 35.9 (2008), pp. 4186–4215.
- [28] Daniel Robinson. “Characterisation of bulk silicon diodes for the magic plate 512 dosimeter array”. PhD thesis. 2013.
- [29] Daniel A. Low et al. “Dosimetry tools and techniques for IMRT”. In: *Medical Physics* 38.3 (2011), pp. 1313–1338.
- [30] Ronald C McGarry et al. “Stereostatic body radiation therapy of early-stage non-small-cell lung carcinoma”. In: *International Journal of Radiation Oncology Biology and Physics* 63.4 (2005), pp. 1010–1015.
- [31] Surendra Rustgi. “Evaluation of the dosimetric characteristics of a diamond detector for photon beam measurements”. In: *Medical Physics* 22.5 (1995), pp. 567–570.
- [32] M Bucciolini et al. “Diamond detector versus silicon diode and ion chamber in photon beams of different energy and field size”. In: *Medical Physics* 30.8 (2003), pp. 2149–2154.
- [33] S Devic et al. “Accurate skin dose measurements using radiochromic film in clinical applications”. In: *Medical Physics* 33.4 (2006), pp. 1116–1124.
- [34] Sami Mohammedsaleh Alshaikh. “MOSFET Annealing and Interface Dosimetry in Complex Radiation Therapy”. PhD thesis. 2012, p. 152.
- [35] Anatoly B. Rosenfeld. “MOSFET Dosimetry On Modern Radiation Oncology Modalities”. In: *Radiation Protection Dosimetry* 101.1-4 (2002), pp. 393–398.
- [36] A Holmes-Siedel. “The Space-Charge Dosimeter - General Principles Of A New Method Radiation Detection”. In: *Nuclear Instruments and Methods in Physics* 121 (1974), pp. 169–179.
- [37] R Freeman and A Holmes-Siedel. “A Simple Model for Predicting Radiation Effects In MOS Devices”. In: *IEEE Transactions on Nuclear Science* 25 (1978), pp. 1216–1225.
- [38] M Petasecca et al. “Angular independent silicon detector for dosimetry in external beam radiotherapy”. In: *Medical Physics* 42.8 (2015), pp. 4708–4718.
- [39] P Metcalfe, T Kron, and P Hoban. *The Physics of Radiotherapy, X-rays and Electrons*. 2007.
- [40] Anthony Anselmo Espinoza. “Development of a silicon detector for dose imaging and measurement in external beam radiotherapy”. PhD thesis. University of Wollongong, 2010, p. 88.
- [41] I. Fuduli et al. “Multichannel Data Acquisition System comparison for Quality Assurance in external beam radiation therapy”. In: *Radiation Measurements* 71 (2014), pp. 338–341.

- [42] Douglas Jones. “ICRU Report 50 - Prescribing, Recording and Reporting Photon Beam Therapy”. In: *Medical Physics* 21.6 (1994), pp. 833–834.
- [43] Glenn F. Knoll. *Radiation Detection and Measurement*. 2000, pp. 86–92.
- [44] R Meiler and M Podgorsak. “Characterisation of the response of commercial diode detectors used for in vivo dosimetry”. In: *Medical Dosimetry* 22.1 (1997), pp. 31–37.
- [45] P Scalchi and P Francescon. “Calibration of a MOSFET detection system for 6-MV in vivo dosimetry”. In: *International Journal of Radiation Oncology Biology and Physics* 40.4 (1998), pp. 987–93.
- [46] G Rikner and E Grusell. “Effects of radiation damage on p-type silicon detectors”. In: *Phys. Med. Biol.* 28.11 (1983), pp. 1261–1267.
- [47] D Georg et al. “Build-up modification of commercial diodes for entrance dose measurements in ‘higher energy’ photon beams.” In: *Radiotherapy Oncology* 51.3 (1999), pp. 249–56.
- [48] J H D Wong et al. “Characterization of a novel two dimensional diode array the ”magic plate” as a radiation detector for radiation therapy treatment.” In: *Medical Physics* 39.5 (2012), pp. 2544–58.
- [49] Marco Petasecca et al. “X-Tream: a novel dosimetry system for Synchrotron Microbeam Radiation Therapy”. In: *Journal of Instrumentation* 31.6 (2015), pp. 568–583.
- [50] Texas Instrument. “64 Channel Analog Front End for Digital X-Ray Detector AFE0064”. In: September (2009).
- [51] Cindy D Smith. “New Method of Collecting Output Factors for Commissioning Linear Accelerators with Special Emphasis on Small Fields and Intensity Modulated Radiation Therapy”. PhD thesis. 2014.
- [52] M Bruzzi et al. “Epitaxial silicon devices for dosimetry applications”. In: *Applied Physics Letters* 90.17 (2007), pp. 10.1063/1.2723075.
- [53] P Cross. “The Use of Parallel Plate Ion Chambers To Determine Surface Dose of a 6MV Photon Beam”. In: *Australasian Physical & Engineering Sciences in Medicine* 15.4 (1992), pp. 208–13.
- [54] Bruce J Gerbi and Faiz M Khan. “Plane-parallel ionisation chamber response in the buildup region of obliquely incident photon beams”. In: *Medical Physics* 24.6 (1997), pp. 873–878.
- [55] B.J Gerbi. “The Response Characteristics Of A Newly Designed Plane-Parallel Ionisation Chamber in High-Energy Photon and Electron Beams”. In: *Medical Physics* 20.5 (1993), pp. 1411–1415.
- [56] Claudiu S Porumb, Dean L Cutajar, and Matthew Newall. “Characterisation of silicon diode arrays for dosimetry in external beam radiation therapy”. In: *IEEE Transactions on Nuclear Science* 63 (2016), pp. 1808–1817.

- [57] PTW. *Small Field Dosimetry Application Guide*. Tech. rep.
- [58] Yuenan Wang, Stephen B. Easterling, and Joseph Y. Ting. “Ion recombination corrections of ionization chambers in flattening filter-free photon radiation.” In: *Journal of applied clinical medical physics / American College of Medical Physics* 13.5 (2012), p. 3758.
- [59] S Agostinelli et al. “Geant4- a simulation toolkit”. In: *Nuclear Instruments and Methods in Physics* 506.3 (2003), pp. 250–303.
- [60] B M Oborn et al. “IMRT treatment Monitor Unit verification using absolute calibrated BEAMnrc and Geant4 Monte Carlo simulations”. In: *Journal of Physics: Conference Series* 489.1 (2014), p. 012020.
- [61] O.A Sauer and J Wilbert. “Measurement of output factors for small photon beams”. In: *Medical Physics* 34.6 (2007), pp. 1983–8.
- [62] Faiz M Khan. *The Physics of Radiation Therapy*. 3rd. Lippincott Williams and Wilkins, 2003.
- [63] I.S Kwan et al. “The effect of rectal heterogeneity on wall dose in high dose rate brachytherapy”. In: *Medical Physics* 36.1 (2008), pp. 224–232.
- [64] Hani Alnawaf, Martin Butson, and Peter K N Yu. “Measurement and effects of MOSKIN detectors on skin dose during high energy radiotherapy treatment”. In: *Australasian Physical and Engineering Sciences in Medicine* 35.3 (2012), pp. 321–328.
- [65] H Jin et al. “Interplay effect of angular dependence and calibration field size of MapCHECK 2 on RapidArc quality assurance”. In: *Journal of Applied Clinical Medical Physics* 15.3 (2014).
- [66] A.H Aldosari et al. “A two-dimensional silicon detectors array for quality assurance in stereotatic radiotherapy: MagicPlate-512”. In: *Medical Physics* 41.9 (2014), p. 091707.
- [67] Fasihah Hanum Yusof et al. “On the use of optically stimulated luminescent dosimeter for surface dose measurement during radiotherapy”. In: *PLoS ONE* 10.6 (2015), pp. 1–15.